Influence of hemoglobin vesicles, cellular-type artificial oxygen carriers, on human umbilical cord blood hematopoietic progenitor cells *in vitro*

Miki Yamaguchi,[1] Mitsuhiro Fujihara,[1] Shinobu Wakamoto,[1] Hiromi Sakai,[2] Shinji Takeoka,[3] Eishun Tsuchida,[2] Hiroshi Azuma,[1] Hisami Ikeda[1]

[1]*Japanese Red Cross, Hokkaido Red Cross Blood Center, Yamanote 2-2, Nishi-Ku, Sapporo 063-0002, Japan*
[2]*Research Institute for Science and Engineering, Waseda University, 3-4-1 Okubo, Shujuku, Tokyo 169-8555, Japan*
[3]*Consolidated Research Institute for Advanced Science and Medical Care, Waseda University, 3-4-1 Okubo, Sinjuku, Tokyo 169–8555, Japan*

Received 25 April 2007; revised 21 August 2007; accepted 16 October 2007
Published online 6 February 2008 in Wiley InterScience (www.interscience.wiley.com). DOI: 10.1002/jbm.a.31857

Abstract: Hemoglobin vesicles (HbVs), liposomal oxygen carriers containing human hemoglobin, are candidates for development as clinically useful blood substitutes. Although HbVs are shown to distribute transiently into the bone marrow in animal models, the influence of HbVs on human hematopoietic stem/progenitor cells has not yet been studied. Therefore, we investigated the influence of HbVs at a concentration of up to 3 vol/vol % on the clonogenic activity (in semisolid culture) and proliferative activity (in liquid culture) of human hematopoietic progenitor cells derived from umbilical cord blood (CB) *in vitro*. Continuous exposure of CB mononuclear cells to HbVs tended to decrease the number and size of mature-committed colonies and most notably reduced the number of colonies of high-proliferative potential colony-forming cells (HPP-CFC). In contrast, exposure to HbVs for 20 h or 3 days, which is more relevant to the clinical setting, had no effect on the number of mature-committed colonies and only modestly decreased the number of HPP-CFC. Continuous exposure (10 days) to HbVs significantly suppressed the cellular proliferation and differentiation of both the erythroid and myeloid lineages in liquid culture. Again, short exposure (20 h or 3 days) did not affect these parameters. Thus, our results show that HbVs, under conditions relevant to the clinical setting, have no adverse effect on human CB hematopoietic progenitor activity *in vitro*.

J Biomed Mater Res 88A: 34–42, 2009

Key words: liposome-encapsulated hemoglobin; hemoglobin-vesicles; hematopoietic progenitor cells; colony assay; biocompatibility

INTRODUCTION

Hemoglobin vesicles (HbVs) or liposome-encapsulated Hbs comprise human hemoglobin encapsulated within a phospholipid bilayer membrane and have been developed as an artificial oxygen carrier.[1–3] Several studies have demonstrated that the HbVs transport oxygen as efficiently as red blood cells,[4–7] making them a promising candidate for clinical trials.

HbVs are injected intravenously, therefore, the biocompatibility of HbVs with blood components is of primary importance to ensure the safety of these materials for clinical use. We have evaluated this biocompatibility by investigating the influence of HbVs on human blood cells as well as plasma *in vitro* and shown that HbVs are highly biocompatible with human blood.[8–10]

It has been clearly demonstrated that intravenously injected liposome products for drug delivery are eventually captured by the reticuloendothelial system (RES), such as Kupffer cells in the liver and macrophages in the spleen and bone marrow.[11] A study in which technetium-99m-labeled HbVs were infused into animals demonstrated that the HbVs were mainly distributed in the liver, spleen and bone marrow,[12] and another histopathological study clarified that the HbVs are promptly metabolized in the RES.[13] Because the clinical utilization of an artificial oxygen carrier as a transfusion alternative would result in the substitution of a large volume of blood,

Correspondence to: M. Fujihara; e-mail: fujihara@hokkaido.bc.jrc.or.jp
Contract grant sponsors: Health and Labor Sciences Research Grants (Research on Regulatory Science of Pharmaceuticals and Medical Devices), Ministry of Health, Labor and Welfare, Japan, and Oxygenix Inc., Tokyo, Japan

it is important to elucidate the influence of HbVs on subsequent hematopoiesis. There has been concern over whether the HbVs distributed into bone marrow might adversely affect hematopoiesis, because the bone marrow is the major site of hematopoiesis. From this point of view, rats that received an acute 40% exchange-transfusion with HbVs showed complete recovery of the hematocrit within 7 days due to the elevated erythropoietic activity.[14] Furthermore, the number of red blood cells, leukocytes, and platelets remained unchanged for 1 week after the infusion of HbVs at 20% of the whole blood volume.[15] The findings in these animal models strongly suggest the absence of inhibitory activity of HbVs against hematopoiesis. However, the influence of HbVs on the human hematopoietic stem/progenitor cells has not yet been studied.

In vitro models of hematopoiesis, such as colony-forming assays, have been widely used to investigate the proliferation and differentiation of both of pluripotent hematopoietic stem cells and different progenitor cells of blood cell lineages [e.g., burst-forming units of erythrocyte (BFU-E) and colony-forming units of granulocytes/macrophages (CFU-GM)]. These techniques appear to be useful for investigating the pathogenic mechanisms of drug-induced blood disorders and also for screening the safety of compounds in preclinical testing.[16]

In this study, therefore, we sought to evaluate the influence of HbVs on the clonogenic activity of human umbilical cord blood (CB) hematopoetic cells, which are rich in hematopoietic stem/progenitor cells. In addition, we investigated the effect of HbVs on the proliferation and differentiation of both the erythroid and myeloid lineages of CB hematopoietic cells in liquid culture.

MATERIAL AND METHODS

HbVs

HbVs were prepared under sterile conditions, as described previously.[17,18] The Hb was purified from outdated donated blood provided by the Japanese Red Cross Society (Tokyo, Japan). The encapsulated Hb solution (38 g/dL) contained 14.7 mmol/L pyridoxal 5′-phosphate (PLP) as an allosteric effector at a molar ratio of [PLP]/[Hb] of 2.5. The lipid bilayer was composed of 1,2-dipalmitoyl-*sn*-glycero-3-phosphatidylcholine, cholesterol, 1,5-*O*-dihexadecyl-*N*-succinyl-L-glutamate (Nippon Fine Chemical, Osaka, Japan), and 1,2-distearoyl-*sn*-glycero-3-phosphatidylethanolamine-*N*-[poly(ethylene glycol) (5,000)] (NOF, Tokyo, Japan) at a molar ratio of 5:5:1:0.033. In some experiments, empty liposomes, which have the same constituents as HbVs, except for the absence of Hb, were used. The concentration of lipopolysaccharide, measured by a modified Limulus test, was less than 0.4 EU/mL.[19] The physicochemical parameters were P_{50}, 27 Torr; 262 ± 77-nm particle diameter; and MetHb content <3%. The concentration of Hb in the HbVs dispersion was adjusted to 10 g/dL. The concentration of HbVs in this study was set at about 3 vol/vol %, based on the following rationale. Intravenously injected HbVs are eventually captured by phagocytes in the RES, including the spleen, liver, and bone marrow. The half-life of HbVs in the circulation in humans has been estimated to be 66 h by the study of circulation kinetics using rats and rabbits,[12] and the percent infused dose of HbVs of bone marrow in humans was estimated to be 6.4% at 48 h after 25% top loading of HbVs, in studies of the organ distribution of HbVs in rats and rabbits.[12] Based on this estimation, the distribution of HbVs in the human bone marrow at 48 h after infusion at 25 vol/vol % (1225 mL of HbVs) of the blood volume (4.9 L, 70 mL/kg, body weight) in a 70-kg individual may be expected to be 78.4 mL (6.4 vol/vol % of the infused dose of HbVs). The volume of the bone marrow space has been estimated as 2.6–4 L in an average-sized human (70 kg).[20] From these values, the amount of HbVs in the human bone marrow can be calculated to be about 2–3 vol/vol %.

Preparation of human CB

Use of human umbilical CB for the experiments was approved by the Committee of Hokkaido CB Bank. CB was obtained during normal full-term deliveries. CB $CD34^+$ cells were prepared as described previously.[21] In brief, after sedimentation of red blood cells by incubating the CB samples with the same volume of 6% (w/v) hydroxyethyl starch dissolved in Ringer's solution (Veen-D, Nikken Chemical, Tokyo, Japan) at room temperature for 30 min, the low-density (<1.077 g/mL) mononuclear cells were collected with Ficoll-Paque (Pharmacia Biotech, Uppsala, Sweden). For some experiments, the cells were further enriched with $CD34^+$ cells using a MACS CD34 Progenitor Isolation Kit (Milenyi Biotech, Bergish-Gladbach, Germany) according to the manufacturer's instructions. In all experiments, the purity of the $CD34^+$ cells was >85%.

Clonal cell culture

The methylcellulose clonal culture was performed in 35-mm suspension culture dishes (Nippon Becton Dickinson [BD], Tokyo, Japan). The population of $CD34^+$ cells among the mononuclear cells was determined by flow cytometry, and the CB-derived mononuclear cells were seeded at 300 $CD34^+$ cells/dish. A complete methylcellulose medium for human clonal culture assays (Methocult GFH4434V; StemCell Technologies, Vancouver BC, Canada) was used. The presence of up to 3% HbVs did not interfere with the microscopic detection of the colonies formed.

After 14 days incubation at 37°C in a humidified atmosphere containing 5% CO_2, the BFU-E, CFU-GM, CFU-Mix, and colony-forming units in culture (CFU-C) were scored under an inverted microscope. Densely packed colonies that reached >1 mm in size were scored as high proliferative potential colony-forming cells (HPP-CFC) after 28 days incubation. In some experiments, the CB-derived

mononuclear cells were suspended to obtain 1500 $CD34^+$ cells/mL in Iscove's modified Dulbecco's medium (IMDM, Gibco BRL, Rockville, MD) containing 30% FCS (Equitech Bio, Igram, TX), 1% bovine serum albumin (BSA; Sigma Chemical, St Louis, MO), 10 ng/mL human interleukin-3 (IL-3), 10 ng/mL human stem cell factor (SCF, provided by Kirin Brewery, Tokyo, Japan), 10 ng/mL granulocyte colony-stimulating factor (G-CSF, a gift from Chugai Pharmaceutical, Tokyo, Japan), and 50 U/mL granulocyte-macrophage colony-stimulating factor (GM-CSF; Schering Research, Bloomfield, NJ). Then, different concentrations of HbVs were added to the cell suspension. The cells were incubated either for 20 h or for 3 days. Subsequently, they were recovered, washed to remove the HbVs, and resuspended in 5 mL of MethoCult GF. One milliliter of the resultant cell suspension (by adjusting $CD34^+$ cells to 300 cells/dish) was seeded into a 35-mm dish for the clonal assay.

Liquid culture

$CD34^+$ cells enriched from CB-derived mononuclear cells were suspended in 4 mL of the following culture media and seeded in 12.5-cm^2 flasks (Nippon BD, Tokyo, Japan). The culture medium for the erythroid lineage was IMDM-containing 30% FBS, 1% BSA, 10 ng/mL human IL-3, 10 ng/mL human SCF, and 2 U/mL human erythropoietin (provided by Chugai Pharmaceutical). The culture medium for the myeloid lineage was IMDM-containing 30% FBS, 1% BSA, 50 μM β-mercaptoethanol, 10 ng/mL human IL-3, 10 ng/mL human SCF, 10 ng/mL G-CSF, and 50 U/mL GM-CSF. These combinations of cytokines have been shown to promote proliferation and differentiation of $CD34^+$ cells toward mature erythroid and myeloid lineage cells, respectively.[22,23] Various concentrations of HbVs were added to the medium containing the cells. After 10 days incubation at 37°C in a humidified atmosphere containing 5% CO_2, the total cell counts were determined. $CD235a^+$ (glycophorin A) cells for the erythroid lineage and $CD15^+$ cells for the myeloid lineage, respectively, were analyzed by flow cytometry. For determining the effects of short-term exposure, the cells were incubated with HbVs for either 20 h or 3 days, washed to remove the HbVs, and then incubated for a total of 10 days.

Flow-cytometric analysis

Aliquots of cells were stained with monoclonal antibodies in PBS/0.1% BSA at 4°C for 30 min. The analysis was performed using a BD LSR flow cytometer (BD Biosciences Immunocytometry System, San Diego, CA). The following monoclonal antibodies were used: FITC-conjugated CD34 (Nippon Becton Dickinson [BD]) antibody, PE-conjugated CD235a and CD33 (DAKO) antibodies, FITC-conjugated CD15 (DAKO) antibody, and APC-conjugated CD45 (BD) antibody. FITC- and PE-conjugated mouse IgG1 antibodies (BD), APC-conjugated mouse IgG1 (BD), and FITC-conjugated IgM (DAKO) antibodies were used as isotype-matched controls. In the flow-cytometric analysis, dead cells were gated out first by propidium iodide staining and then with a forward versus side scatter window. For each analysis set, at least 10,000 events were collected.

Histological staining

Cultured cells ($1 \times 10^3 - 1 \times 10^4$/100 μL) were centrifuged onto slides with Cytospin (Shandon, Pittsburgh, PA) and stained with May-Grünwald-Giemsa (Merck, Darmstadt, Germany). Microscopic images were captured with an MP5Mc/OL digital camera (Olympus) and processed using Win Roof software, version 5.5.

Statistical analysis

Results are expressed as mean ± standard deviation (SD). A two-way paired ANOVA followed by *post hoc* Bonferroni's test was used for comparisons of multiple HbV-treated groups with the control (HbV; 0%) group. For analysis of the difference between two exposure times, unpaired two-tailed Student's t test was used. Values of $p < 0.05$ were considered significant.

RESULTS AND DISCUSSION

Clonogenic potential of CB hematopoietic cells

We first examined the effect of continuous exposure to HbVs (0.09%–3%) on the formation of BFU-E, CFU-GM, CFU-Mix, CFC, and HPP-CFC in the clonogenic assay. HbVs at 3% inhibited the formation of CFU-GM and tended to decrease the formation of CFC-C. Most notably, HbVs significantly inhibited the formation of HPP-CFC in a concentration-dependent manner (Fig. 1A). Although no change in the number of colonies of BFU-E was noted, the size of the colonies of BFU-E and CFU-GM tended to be smaller in the presence than in the absence of HbVs (Fig. 2). On the other hand, the empty liposomes (phospholipid vesicles devoid of Hb) had no inhibitory effect on the formation of mature-committed colonies or HPP-CFC (Fig. 1B).

As continuous exposure to HbVs had a marked inhibitory effect on the formation of HPP-CFC, we examined the effect of short-term exposure of CB hematopoietic cells to HbVs. Toward this end, the CB hematopoietic cells were exposed to HbVs for 20 h or for 3 days, washed to remove the HbVs, and then subjected to a clonogenic assay. Exposure to HbVs for 20 h had no inhibitory effect on the formation of either HPP-CFC or other mature-committed colonies (Fig. 3). Exposure to 3% HbVs for 3 days modestly inhibited the formation of HPP-CFC, however, a greater number of HPP-CFC was formed when compared with that observed under continuous exposure to HbVs. No effect was observed on the formation of

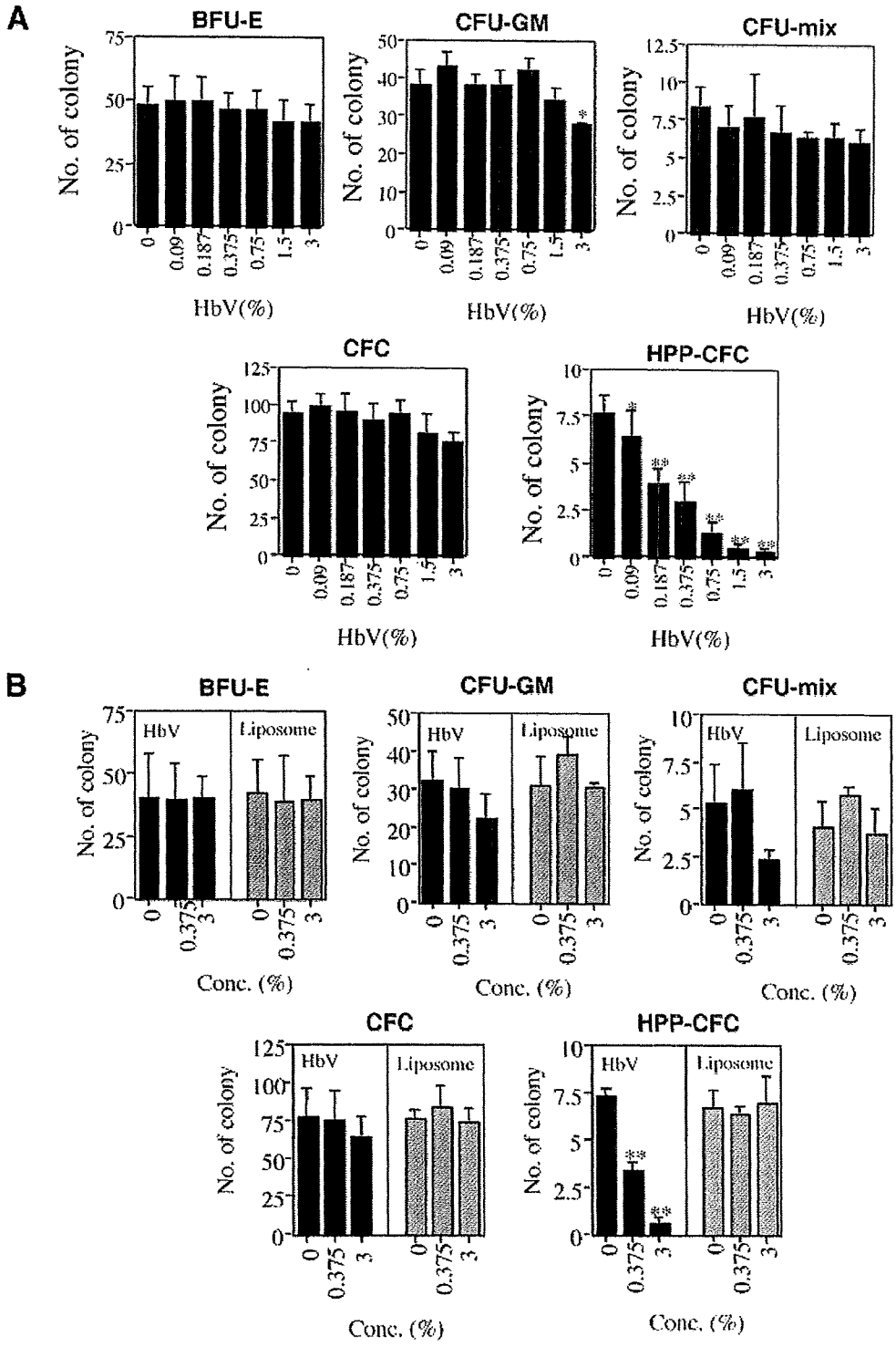

Figure 1. A: Effects of HbVs on the clonogenic activity of CB-derived hematopoietic cells. B: Effects of empty liposomes on the clonogenic activity of CB-derived hematopoietic cells. CB-derived mononuclear cells were seeded at 300 $CD34^+$ cells per dish in complete methylcellulose medium for human clonal-culture assays. Various concentrations of HbVs or empty liposomes (vol/vol %) were added to the medium containing the cells. BFU-E, CFU-GM, CFU-Mix, and CFU-C were scored after 14 days incubation. HPP-CFC was scored after 28 days incubation. Data represent the mean ± SD of three experiments performed on three separate CB donors in (A) and (B), respectively. A two-way paired ANOVA followed by Bonferroni's test was used for comparisons of multiple HbVs-treated groups with the control (HbVs; 0%) group. $^*p < 0.05$, $^{**}p < 0.01$ versus HbVs (0%).

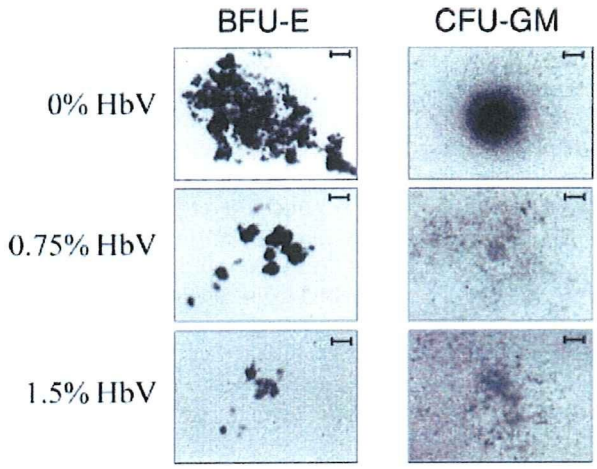

Figure 2. Effects of HbVs on the size of the colonies of BFU-E and CFU-GM formed in clonal cultures of CB-derived cells. Representative colonies of BFU-E and CFU-GM in the absence and presence of HbVs are shown. Scales represent 50 μm.

other mature-committed colonies (Fig. 3). From the clinical point of view, continuous exposure of hematopoietic stem/progenitor cells to HbVs in the marrow for 14 days or 28 days is unlikely. Rather, 1–3 days exposure is more relevant to the clinical setting as described below. In this sense, short-term exposure of hematopoietic progenitor cells to HbVs even at 3% had no adverse effect on the clonogenic activity of hematopoietic progenitor cells.

Proliferation and differentiation of erythroid or myeloid lineage cells from CB hematopoietic progenitor cells in liquid culture

Because the numbers of HPP-CFC and CFU-GM were significantly reduced, and the size of the colonies of BFU-E and CFU-GM tended to be smaller in the presence than in the absence of HbVs, we next examined the effect of HbVs (0.75%, 1.5%, or 3%) on the proliferation of erythroid or myeloid lineage cells in a liquid culture of CB $CD34^+$ cells. As shown in Figure 4, the presence of HbVs throughout the culture period significantly inhibited the proliferation of $CD235a^+$ cells (erythroid lineage) and $CD15^+$ (myeloid lineage) cells in a dose-dependent manner. These results suggested that continuous exposure to HbVs had an inhibitory effect on the proliferation of hematopoietic progenitor cells. Thus, the reduced number of HPP-CFC and reduced colony size of BFU-E and CFU-GM in the clonogenic assay were surmised to be associated with reduced proliferation of the erythroid and myeloid lineage cells in the presence of HbVs throughout the culture period.

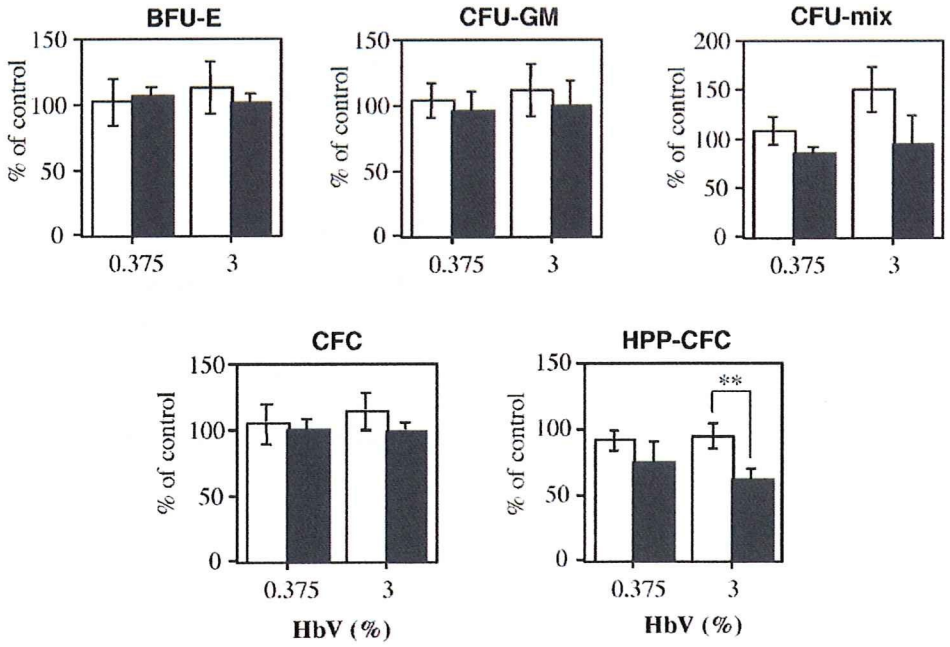

Figure 3. Effects of short-term exposure to HbVs on the clonogenic activity of CB-derived hematopoietic cells. CB-derived mononuclear cells were suspended in IMDM containing FCS, BSA, IL-3, SCF, G-CSF, and GM-CSF; then, different concentrations of HbVs were added to the cell suspension. The cells were incubated for 20 h (open column) or for 3 days (closed column). Subsequently, they were recovered, washed to remove the HbVs, and subjected to clonal assay. Data were expressed as the mean ± SD of the percentage of control. Three experiments were performed on three separate CB donors. $^{**}p < 0.01$; 20 h versus 3-day exposure; unpaired Student's t test.

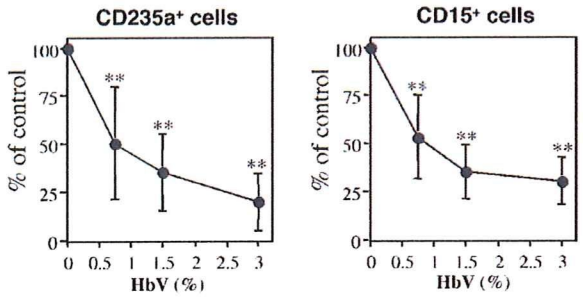

Figure 4. Effects of HbVs on the proliferation of erythroid lineage (left panel) or myeloid lineage cells (right panel) from CB-derived hematopoietic progenitor cells in liquid culture. Various concentrations of HbVs were added to medium containing the CB-derived $CD34^+$ cells. After 10 days' incubation, $CD235a^+$ cells for the erythroid lineage and $CD15^+$ cells for the myeloid lineage, respectively, were analyzed by flow cytometry. Data represent the mean ± SD of six experiments performed on six separate CB donors. A two-way paired ANOVA followed by Bonferroni's test was used for comparisons of multiple HbVs-treated groups with the control (HbVs; 0%) group. $^{**}p < 0.01$ versus HbVs (0%).

We further analyzed the subset of $CD235a^+$ cells and $CD15^+$ cells. The $CD235a^+CD45^-$ cells and $CD15^+CD33^-$ cells represented some of the more differentiated cells in the erythroid and myeloid lineage, respectively. Continuous exposure to HbVs significantly reduced the percentage of $CD233^+CD45^-$ cells in the total cell population (Fig. 5A). Microscopic examination of a smear of cells cultured for 10 days revealed that while orthochromatic erythroblasts and erythrocytes (differentiated lineage) were present in the absence of HbVs, basophilic erythroblasts (less differentiated lineage) were more abundant in the presence of 3% HbVs (Fig. 5B).

Similarly, continuous exposure to HbVs significantly decreased the percentage of $CD15^+CD33^-$ cells in the total cell population (Fig. 6A). Examination of a smear of the cells showed that while metamyelocytes (differentiated lineage) could be recognized in the absence of HbVs, myelocytes (less differentiated lineage) were more abundant in the presence of 3% HbVs (Fig. 6B). These results suggest that continuous exposure to HbVs also inhibited the

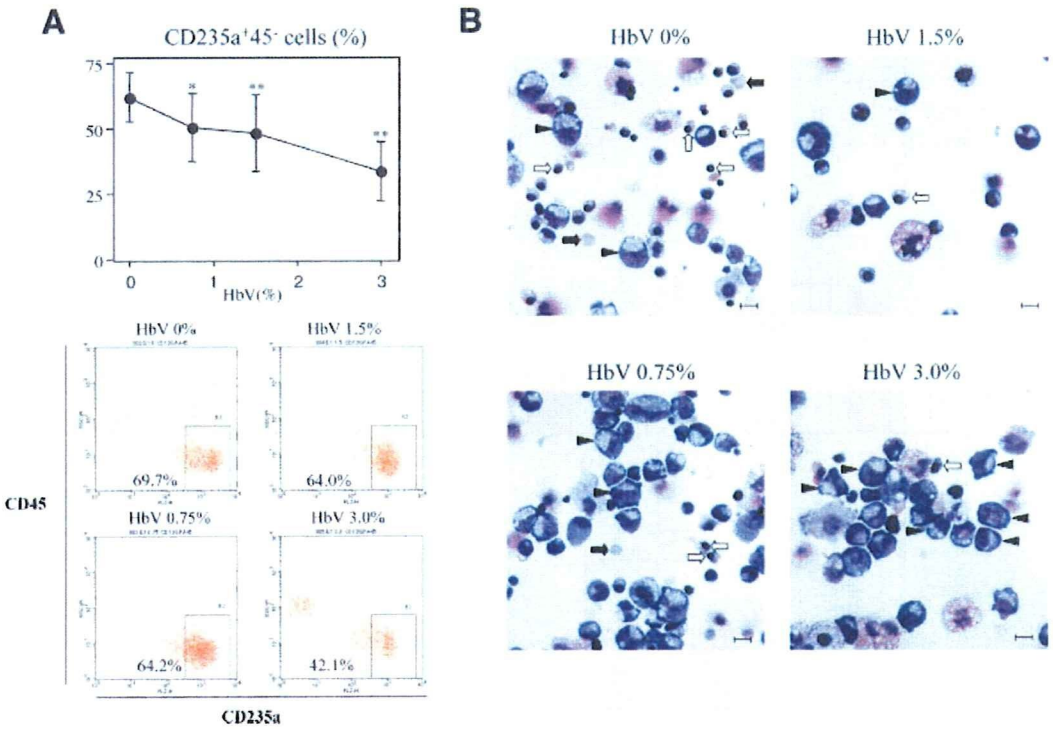

Figure 5. Effects of HbVs on the differentiation of erythroid cells from CB-derived hematopoietic progenitor cells in liquid culture. CB-derived $CD34^+$ cells were cultured in the medium for induction of erythroid lineage without or with HbVs (0.75%, 1.5%, or 3.0%). A: The percentage of $CD235a^+$ $CD45^-$ cells in the total cell population was analyzed by flow cytometry. Data represent the mean ± SD of experiments performed on CB obtained from six separate donors. A two-way paired ANOVA followed by Bonferroni's test was used for comparisons of multiple HbVs-treated groups with the control (HbVs 0%) group. $^*p < 0.05$, $^{**}p < 0.01$ versus HbVs (0%). Representative results of flow cytometric analysis are shown at the bottom. B: Morphology of the cells generated in the liquid culture for erythroid lineage. Arrow head; basophilic erythroblasts, white arrow; orthochromatic erythroblasts, and black arrow; erythrocyte. Note that the differentiated erythroid cells are much fewer in number in the presence of HbVs when compared with that in the control (HbVs 0%). [Color figure can be viewed in the online issue, which is available at www.interscience.wiley.com.]

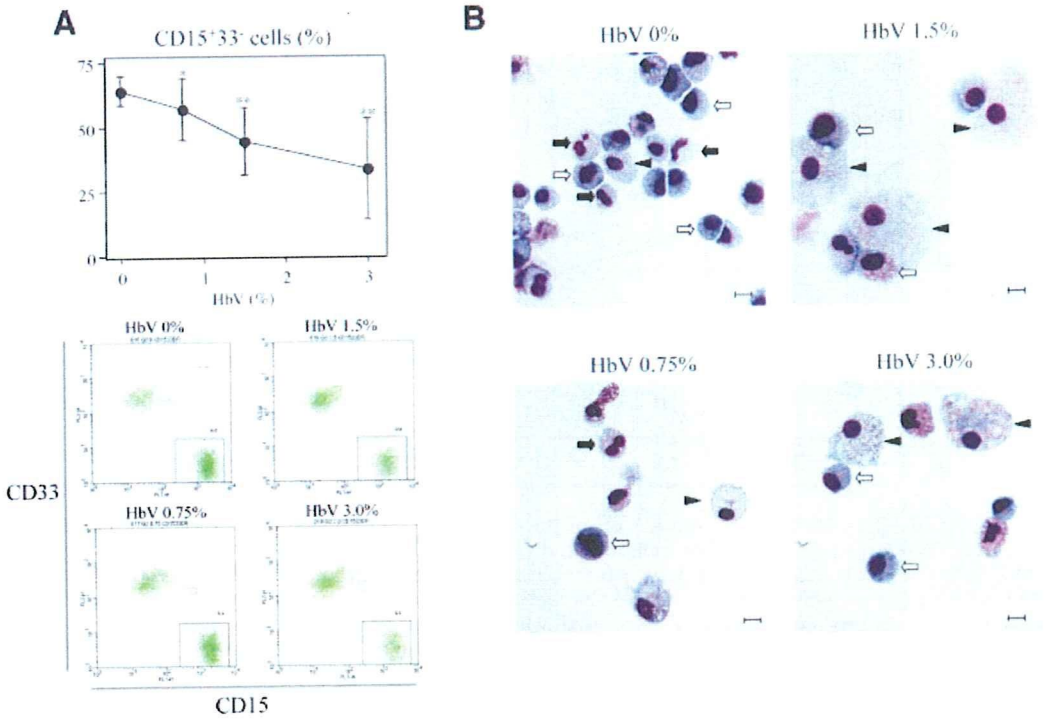

Figure 6. Effects of HbVs on the differentiation of myeloid cells from CB-derived hematopoietic progenitor cells in liquid culture. CB-derived $CD34^+$ cells were cultured in the medium for the induction of myeloid lineage without or with HbVs (0.75%, 1.5% or 3.0%). A: The percentage of $CD15^+$ $CD33^-$ cells in the total cell population was analyzed by flow cytometry. Data represent the mean ± SD of experiments performed on six separate CB donors. A two-way paired ANOVA followed by Bonferroni's test was used for the comparisons of multiple HbVs-treated groups with the control (HbVs 0%) group. $^*p < 0.05$, $^{**}p < 0.01$ versus HbVs (0%). Representative results of flow cytometric analysis are shown at the bottom. B: Morphology of the cells generated in the liquid culture for erythroid lineage. Arrow head, macrophage; white arrow, myelocyte; and black arrow, metamyelocyte. Note that the differentiated myeloid cells are much fewer in number in the presence of HbVs when compared with that in the control (HbVs 0%). Scales represent 10 μm. [Color figure can be viewed in the online issue, which is available at www.interscience.wiley.com.]

differentiation of both erythroid and myeloid lineage cells.

Next, the effects of the short exposure to HbVs, which is more relevant to the clinical setting, of $CD34^+$ cells on the proliferative activity of both erythroid and myeloid lineage cells were examined. Exposure to HbVs even at 3% for 20 h or for 3 days did not affect the proliferative activity of either the $CD235a^+$ cells or the $CD15^+$ cells (Fig. 7). Furthermore, the percentages of $CD235a^+CD45^-$ cells and $CD15^+CD33^-$ cells in the total cell population were not affected by exposure to HbVs, either for 20 h or for 3 days (data not shown). Thus, HbVs exerted no inhibitory effects on the proliferation and differentiation of either erythroid or myeloid lineage cells following short durations of exposure.

Several hypotheses have been suggested to explain the inhibitory effects of continuous exposure to HbVs on hematopoietic progenitor activity including direct contact of the progenitor cells with HbVs, conversion of Hb in HbVs to met-Hb during culture, interaction of progenitor cells with several components from HbVs, which might degrade over time. The observation that the empty liposomes did not have any inhibitory effect on the clonogenic activity suggested that the progenitor activity was not inhibited by direct contact of the progenitor cells with the HbVs surface, but by the presence of Hb in the HbVs. In this case, higher dissolved oxygen concentrations in the culture medium were theoretically expected in the presence of HbVs than in the absence of HbVs, which may be involved in the inhibition of progenitor activity following to the prolonged exposure to HbVs. Furthermore, conversion of Hb to met-Hb within HbVs[24] cannot be excluded as the reason for the inhibition of progenitor activity caused by HbVs. In addition, there is a possibility that HbVs might degrade during long-term incubation, leading to the release of Hb. We determined the Hb level during the continuous presence of HbVs in liquid culture up to 10 days. At maximum, 6.7% of the Hb in the HbVs inputted at 3% (i.e., 0.02

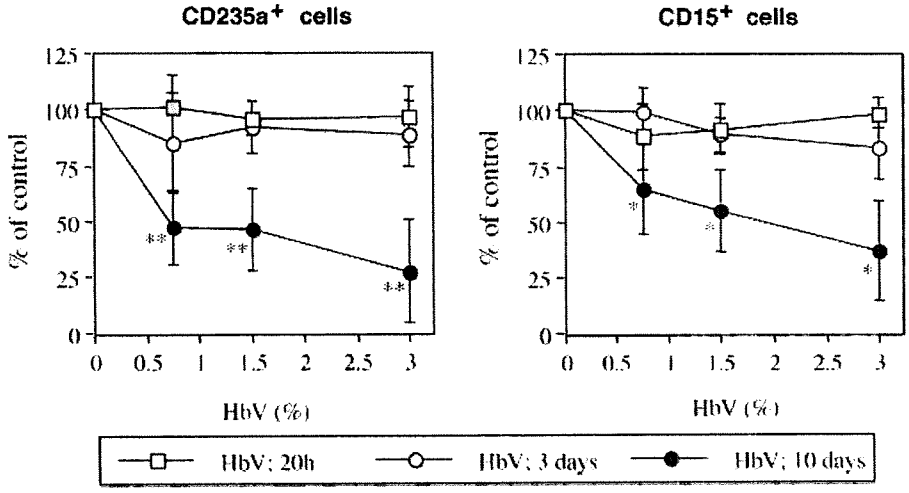

Figure 7. Effects of HbVs on the proliferation of erythroid lineage (left panels) or myeloid lineage (right panels) cells from CB-derived hematopoietic progenitor cells in liquid culture. CB-derived $CD34^+$ cells were exposed to HbVs (0%, 0.75%, 1.5%, or 3%) for 20 h, 3 days, or 10 days. After culture for a total of 10 days, $CD235a^+$ cells for the erythroid lineage and $CD15^+$ cells for the myeloid lineage, respectively, were analyzed by flow cytometry. The number of $CD235a^+$ cells or $CD15^+$ cells at each concentration of HbVs is expressed as a percentage of the number in the control (HbVs 0%). Data represent the mean ± SD of three experiments performed on three separate CB donors. A two-way paired ANOVA followed by Bonferroni's test was used for comparisons of multiple HbVs-treated groups with the control (HbVs 0%) group. $*p < 0.05$, $**p < 0.01$ versus HbVs (0%).

g/dL) was released into the culture supernatant. This Hb concentration was calculated as ~3 μ*M*. According to the report by Fowler et al.,[25] 1 μ*M* of recombinant Hb did not affect the proliferation of erythroid or myeloid lineage cells from human bone marrow $CD34^+$ cells in liquid culture system. Therefore, we do not believe that the released Hb accounted for the inhibitory effect of long-term exposure to HbVs on the progenitor activity.

It is difficult to predict the events *in vivo* from the results of experiments *in vitro*, because the effects of HbVs on the immature hematopoietic stem/progenitor cells from the CB may not be the same as those on the hematopoietic stem/progenitor cells in the adult bone marrow. In addition, the concentration of HbVs used here is based on simple assumption and may not necessarily be relevant to the physiological conditions prevailing in humans. With regard to the exposure time to HbVs, continuous exposure of hematopoietic stem/progenitor cells to HbVs in the marrow for more than 10 days is unlikely in the clinical setting. Rather, 1–3 days exposure is more relevant to the clinical setting, because a study in which an acute 40% exchange transfusion of HbVs was administered to rats showed that a significant amount of the HbVs was phagocytosed by the macrophages in the marrow by 1–3 days after the infusion. A significant decrease in the number of HbVs was observed at 7 days, with the vesicles becoming undetectable at 14 days. Under these conditions, hematopoietic activity, including the formation of erythroblastic islets was observed at 3 days in the marrow.[14] Moreover, the destination of HbVs in the bone marrow is macrophages, and the HbVs are degraded in the phagosomes. These findings imply that there is little possibility of direct contact between HbVs and the hematopoietic progenitor cells *in vivo*. The finding that short-term exposure to HbVs did not have any significant effect on the clonogenic activity or the proliferation and differentiation of erythroid and myeloid lineage cells in liquid culture is consistent with the results of animal experiments,[14,15] suggesting that the infusion of HbVs in humans may have no adverse effects on hematopoiesis.

In conclusion, our results suggest that HbVs, under conditions relevant to the clinical setting, have no adverse effect on human CB hematopoietic progenitor activity *in vitro*. The present results are of value for estimating the biocompatibility of HbVs and hematopoietic progenitor cells.

The authors thank Prof. Koichi Kobayashi and Dr. Hirohisa Horinouchi (School of Medicine, Keio University) for their meaningful discussions.

References

1. Djordjevich L, Miller IF. Synthetic erythrocytes from lipid encapsulated hemoglobin. Exp Hematol 1980;8:584–592.

2. Phillips WT, Klipper RW, Awasthi VD, Rudolph AS, Cliff R, Kwasiborski V, Goins BA. Polyethylene glycol-modified liposome-encapsulated hemoglobin: A long circulating red cell substitute. J Pharmacol Exp Ther 1999;288:665–670.
3. Chang TM. Hemoglobin-based red blood cell substitutes. Artif Organs 2004;28:789–794.
4. Sakai H, Takeoka S, Park SI, Kose T, Nishide H, Izumi Y, Yoshizu A, Kobayashi K, Tsuchida E. Surface modification of hemoglobin vesicles with poly(ethylene glycol) and effects on aggregation, viscosity, and blood flow during 90% exchange transfusion in anesthetized rats. Bioconjugate Chem 1997;8:23–30.
5. Sakai H, Masada Y, Horinouchi H, Yamamoto M, Ikeda E, Takeoka S, Kobayashi K, Tsuchida E. Hemoglobin-vesicles suspended in recombinant human serum albumin for resuscitation from hemorrhagic shock in anesthetized rats. Crit Care Med 2004;32:539–545.
6. Cabrales P, Sakai H, Tsai AG, Takeoka S, Tsuchida E, Intaglietta M. Oxygen transport by low and normal oxygen affinity hemoglobin vesicles in extreme hemodilution. Am J Physiol Heart Circ Physiol 2005;288:H1885–H1892.
7. Yoshizu A, Izumi Y, Park S, Sakai H, Takeoka S, Horinouchi H, Ikeda E, Tsuchida E, Kobayashi K. Hemorrhagic shock resuscitation with an artificial oxygen carrier, hemoglobin vesicle, maintains intestinal perfusion and suppresses the increase in plasma tumor necrosis factor-α. ASAIO J 2004;50:458–463.
8. Wakamoto S, Fujihara M, Abe H, Yamaguchi M, Azuma H, Ikeda H, Takeoka S, Tsuchida E. Effects of hemoglobin vesicles on resting and agonist-stimulated human platelets in vitro. Artif Cells Blood Subs Biotechnol 2005;33:101–111.
9. Ito T, Fujihara M, Abe H, Yamaguchi M, Wakamoto S, Takeoka S, Sakai H, Tsuchida E, Ikeda H, Ikebuchi K. Effects of poly(ethyleneglycol)-modified hemoglobin vesicles on *N*-formyl-methionyl-leucyl-phenylalanine-induced responses of polymorphonuclear neutrophils in vitro. Artif Cells Blood Substit Immobil Biotechnol 2001;29:427–437.
10. Abe H, Fujihara M, Azuma H, Ikeda H, Ikebuchi K, Takeoka S, Tsuchida E, Harashima H. Interaction of hemoglobin vesicles, a cellular-type artificial oxygen carrier, with human plasma: Effects on coagulation, kallikrein-kinin, and complement systems. Artif Cells Blood Substit Immobil Biotechnol 2006;34:1–10.
11. Torchilin VP. Recent advances with liposomes as pharmaceutical carriers. Nat Rev Drug Discov 2005;4:145–160.
12. Sou K, Klipper R, Goins B, Tsuchida E, Phillips WT. Circulation kinetics and organ distribution of Hb-vesicles developed as a red blood cell substitute. J Pharmacol Exp Ther 2005;312:702–709.
13. Sakai H, Horinouchi H, Tomiyama K, Ikeda E, Takeoka S, Kobayashi K, Tsuchida E. Hemoglobin-vesicles as oxygen carriers: Influence on phagocytic activity and histopathological changes in reticuloendothelial system. Am J Pathol 2001;159:1079–1088.
14. Sakai H, Horinouchi H, Yamamoto M, Ikeda E, Takeoka S, Takaori M, Tsuchida E, Kobayashi K. Acute 40 percent exchange-transfusion with hemoglobin-vesicles (HbV) suspended in recombinant human serum albumin solution: Degradation of HbV and erythropoiesis in a rat spleen for 2 weeks. Transfusion 2006;46:339–347.
15. Abe H, Azuma H, Yamaguchi M, Fujihara M, Ikeda H, Sakai H, Takeoka S, Tsuchida E. Effects of hemoglobin vesicles, a liposomal artificial oxygen carrier, on hematological responses, complement and anaphylactic reactions in rats. Artif Cells Blood Substit Immobil Biotechnol 2007;35:157–172.
16. Pessina A, Malerba I, Gribaldo L. Hematotoxicity testing by cell clonogenic assay in drug development and preclinical trials. Curr Pharm Des 2005;11:1055–1065.
17. Sakai H, Yuasa M, Onuma H, Takeoka S, Tsuchida E. Synthesis and physicochemical characterization of a series of hemoglobin-based oxygen carriers: Objective comparison between cellular and acellular types. Bioconjugate Chem 2000;11:56–64.
18. Sou K, Naito Y, Endo T, Takeoka S, Tsuchida E. Effective encapsulation of proteins into size-controlled phospholipid vesicles using freeze-thawing and extrusion. Biotechnol Prog 2003;19:1547–1552.
19. Sakai H, Hisamoto S, Fukutomi I, Sou K, Takeoka S, Tsuchida E. Detection of lipopolysaccharide in hemoglobin-vesicles by Limulus amebocyte lysate test with kinetic-turbidimetric gel clotting analysis and pretreatment of surfactant. J Pharm Sci 2004;93:310–321.
20. Lipton JM, Nathan DG. The anatomy and physiology of hematopoiesis. In: Nathan DG, Oski FA, editors. Hematology of Infancy and Childhood. Philadelphia: WB Saunders; 1987. p 128–158.
21. Ohkawara JI, Ikebuchi K, Fujihara M, Sato N, Hirayama F, Yamaguchi M, Mori KJ, Sekiguchi S. Culture system for extensive production of CD19+IgM+ cells by human cord blood CD34+ progenitors. Leukemia 1998;12:764–771.
22. Giarratana MC, Kobari L, Lapillonne H, Chalmers D, Kiger L, Cynober T, Marden MC, Wajcman H, Douay L. Ex vivo generation of fully mature human red blood cells from hematopoietic stem cells. Nat Biotechnol 2005;23:69–74.
23. Unverzagt KL, Bender JG, Loudovaris M, Martinson JA, Hazelton B, Weaver C. Characterization of a culture-derived CD15+CD11b- promyelocytic population from CD34+ peripheral blood cells. J Leukoc Biol 1997;62:480–484.
24. Teramura Y, Kanazawa H, Sakai H, Takeoka S, Tsuchida E. Prolonged oxygen-carrying ability of hemoglobin vesicles by coencapsulation of catalase in vivo. Bioconjugate Chem 2003;14:1171–1176.
25. Fowler DA, Rsosenthal GJ, Sommadossi JP. Effect of recombinant human hemoglobin on human bone marrow progenitor cells: protection and reversal of 3′-azido-3′-deoxythymidine-induced toxicity. Toxicol Lett 1996;85:55–62.

Nitric Oxide xxx (2009) xxx–xxx

Contents lists available at ScienceDirect

Nitric Oxide

journal homepage: www.elsevier.com/locate/yniox

Nitrosylated human serum albumin (SNO-HSA) induces apoptosis in tumor cells ☆

Naohisa Katayama [a,b], Keisuke Nakajou [b], Yu Ishima [a], Shotaro Ikuta [b], Jun-ichi Yokoe [b], Fumika Yoshida [a], Ayaka Suenaga [a], Toru Maruyama [a,c], Toshiya Kai [a,b], Masaki Otagiri [a,d,*]

[a] Department of Biopharmaceutics, Graduate School of Pharmaceutical Sciences, Kumamoto University, 5-1 Oe-honmachi, Kumamoto 862-0973, Japan
[b] Pharmaceutical Research Center, Nipro 3023 Nojicho, Kusatsu, Shiga 525-0055, Japan
[c] Department of Clinical Pharmaceutics, Graduate School of Sciences, Kumamoto University, 5-1 Oe-honmachi, Kumamoto 862-0973, Japan
[d] Faculty of Pharmaceutical Sciences, Sojo University, 4-22-1 Ikeda, Kumamoto 860-0082, Japan

ARTICLE INFO

Article history:
Received 27 June 2009
Revised 19 September 2009
Available online xxxx

Keywords:
SNO-HSA
Nitric oxide
Apoptosis
Anti-tumor effect
Cancer
Nitrosylation

ABSTRACT

Recently, nitric oxide has been investigated as a potential anti-cancer therapy because of its cytotoxic activity. Previously, we found that S-nitrosylated human serum albumin (SNO-HSA) induced apoptosis in C26 cells, demonstrating for the first time that SNO-HSA has potential as an anti-cancer drug. In the present study, the anti-tumor activity of SNO-HSA in another tumor type of cancer cell was investigated using murine tumor LY-80 cells. Mitochondrial depolarization, activation of caspase-3 and DNA fragmentation were induced in LY-80 cells by SNO-HSA treatment in a dose-dependent manner. Inhibition of caspase activity resulted in complete inhibition of DNA fragmentation induced by SNO-HSA. The cytotoxic effects of SNO-HSA on LY-80 were concentration-dependent. Tumor growth in LY-80-tumor-bearing rats was significantly inhibited by administration of SNO-HSA compared with saline- and HSA-treatment. These results suggest that SNO-HSA has potential as a chemopreventive and/or chemotherapeutic agent because it induces apoptosis in tumor cells.

Introduction

Somatic cells are generated by mitosis and almost all will die by apoptosis-physiologic cell suicide. Malignant growth occurs when this balance is disturbed due to either an increase in cellular proliferation or a decrease in cell death. There is a growing awareness that many of the changes that contribute to the development of cancers also interfere with apoptosis [1]. Therefore, induction of apoptosis in neoplastic cells effectively results in tumor eradication [2]. However, this type of chemotherapy often has negative side effects, such as transient cell cycle arrest, senescence, and autophagy. Drug delivery systems that facilitate selective apoptosis of neoplastic cells have been suggested as a way to overcome this problem [3,4].

Nitric oxide (NO)[1] is a unique, diffusible molecular messenger that plays a central role in mammalian pathophysiology [5]. The effects of NO are pleiotropic: vascular smooth muscle relaxation [6,7], inhibition of platelet aggregation [8], effects on neurotransmission [9], and regulation of immune function [10]. However, under some circumstances, NO is cytotoxic [11]. In L10 hepatoma cells, NO causes cellular iron loss, and inhibits DNA synthesis, mitochondrial respiration, and aconitase activity [12]. In addition, NO reacts with superoxide anion (which is produced by activated macrophages and other cells) to form peroxynitrite. This byproduct of NO is a potent chemical oxidant, which alters protein function and damages DNA [13]. These effects are part of the nonspecific host defense system, which facilitates killing of tumor cells and intracellular pathogens. In addition, the cytotoxic effects of long-lived NO result from induction of apoptosis [5]. In particular, high concentrations of NO inhibit tumor cell growth and induce apoptosis [14]. However, the half-life of NO *in vivo* (~0.1 s) is so short that NO itself cannot be used as a therapeutic agent. Recently, NO-donating non-steroidal anti-inflammatory drugs (NO-NSAIDs), in particular NO-aspirin (NO-ASA), have been investigated as promising chemopreventive agents [15–17]. NO-ASA consists of traditional ASA to which a NO-releasing moiety is bound via a spacer.

Previously, we selected human serum albumin (HSA) as the NO-carrier. S-nitrosylated HSA appears to act as a reservoir of NO *in vivo* [18] and, therefore, is expected to be a clinically feasible biocompatible pharmacological agent. One molecule of HSA contains 35 cysteine residues. However 34 of them form 17 non-reactive disulfide bonds, and thus only one residue (Cys-34) forms a reactive free thiol for S-nitrosylation [19]. Consequently, we increased the number of free sulfhydryl groups on HSA. HSA was reacted with

☆ SNO-HSA induces apoptosis in tumor cells.

* Corresponding author. Fax: +81 96 362 7690.
E-mail address: otagirim@gpo.kumamoto-u.ac.jp (M. Otagiri).

[1] *Abbreviations:* NO, nitric oxide; SNO-HSA, nitrosylated human serum albumin; rHSA, recombinant human serum albumin; NO-NSAID, nitric oxide-donating non-steroidal anti-inflammatory drug; NO-ASA, nitric oxide-donating aspirin; DTPA, diethylenetriaminepentaacetic acid; LDH, lactate dehydrogenase; BSA, bovine serum albumin; R410C, genetic variant of human serum albumin mutated at position 410.

1089-8603/$ - see front matter © 2009 Published by Elsevier Inc.
doi:10.1016/j.niox.2009.09.003

iminothiolane to produce poly S-nitrosylated HSA (SNO-HSA, 6.6 mol SNO/mol HSA). SNO-HSA induced oxidative stress and apoptosis via activation of the intrinsic apoptosis pathway in murine colon 26 carcinoma (C26) cells *in vitro*. Furthermore, intravenous administration of SNO-HSA inhibited tumor growth in C26 tumor-bearing mice, due to its pro-apoptosis effects [20].

In the present study, the anti-tumor activity of SNO-HSA was evaluated extensively using a rat tumor cell line-LY-80 (a variant of Yoshida sarcoma). The LY-80 cell line is a non-adherent cell type that can be implanted into the rat; thus LY-80 cells have been utilized for cancer research. The molecular events by which SNO-HSA induces apoptosis were studied *in vitro* and the anti-tumor activity of SNO-HSA was studied *in vivo* using a rat model of LY-80 sarcoma.

Materials and methods

Chemicals

Traut's Reagent (2-imminothiolane) was purchased from Pierce Chemical Co. (Rockford, IL, USA). Isopentyl nitrite, diethylenetriaminepentaacetic acid (DTPA) and a Cell Counting Kit-8 were purchased from Wako Pure Chemical Industries, Ltd. (Osaka, Japan). RPMI-1640 medium and RNase A were obtained from Sigma Chemical (St. Louis, MO, USA). Proteinase K was obtained from Roche Applied Science (Indianapolis, IN, USA). All other reagents were the highest grade available from commercial sources.

Expression and purification of recombinant human serum albumin (rHSA)

rHSA was produced using a yeast expression system as described previously [21]. Briefly, to construct the HSA expression vector, pPIC9-HSA, a native HSA coding region was incorporated into the methanol-inducible pPIC9 vector (Invitrogen Co., San Diego, CA, USA). The resulting vector was introduced into the yeast species, *P. pastoris* (strain GS115), for expression of rHSA. Secreted rHSA was isolated from the growth medium by both precipitation with 60% (w/v) $(NH_4)_2SO_4$ and purification on a Blue Sepharose CL-6B column (GE Healthcare, Buckinghamshire, England) and then on a Phenyl HP column (GE Healthcare, Buckinghamshire, England). The isolated protein was defatted using the charcoal procedure described by Chen [22], deionized, freeze-dried and then stored at −20 °C until use. The resulting rHSA (treated with dithiothreitol) exhibited a single band on SDS/PAGE. Density analysis of protein bands stained with Coomassie brilliant blue revealed the final produce was ⩾97% pure.

Synthesis of HSA (I), SNO-HSA and SNO-HSA (R)

Terminal sulfhydryl groups were added to the HSA molecule by incubation of 0.15 mM rHSA with 3 mM Traut's Reagent (2-imminothiolane) in 100 mM potassium phosphate buffer containing 0.5 mM DTPA (pH 7.8) for 1 h at room temperature. The resultant modified rHSA then was divided into two portions, after that one was concentrated, exchanged with saline and adjusted to 2 mM, designated as HSA (I), the other was S-nitrosylated via 3 h incubation with 15 mM isopentyl nitrite at room temperature. The resulting SNO-HSA was concentrated and exchanged with saline using a PelliconXL filtration device (Millipore Corporation, Billerica, MA, USA). The final concentration was adjusted to 2 mM SNO-HSA and the sample was stored at −80 °C until use.

In order to obtain free sulfhydryl groups on HSA molecule, 0.3 mM HSA was incubated with 30 mM dithiothreitol in 200 mM Tris–HCl buffer containing 1 mM EDTA and 8 M urea (pH 8.2) for 4 h at room temperature. Dithiothreitol was then quickly removed by Sephadex G-25 gel filtration and eluted with 100 mM acetic acids. Then, 0.1 mM reduced HSA was incubated with 10 mM isoamyl nitrite in 100 mM potassium phosphate buffer containing 0.5 mM DTPA (pH 7.8) for 1 h at room temperature, followed by Sephadex G-25 gel filtration, concentration and exchange with saline to 2 mM SNO-HSA (R). The sample was stored at −80 °C until use.

The number of the S-nitroso moieties on SNO-HSA and SNO-HSA (R) were determined using a 96-well plate. First, 20-μl aliquots of sample solutions and $NaNO_2$ (standard) were incubated with 0.2 ml of 10 mM sodium acetate buffer (pH 5.5) containing 100 mM NaCl, 0.5 mM DTPA, 0.015% N-1-naphthylsthylene-diamide and 0.15% sulfanilamide with or without 0.09 mM $HgCl_2$ for 30 min at room temperature. Then, absorbance at 540 nm was measured. The number of moles of NO per mole of HSA was estimated by subtracting the values obtained in the absence of $HgCl_2$ from those measured in the presence of $HgCl_2$; the values obtained from SNO-HSA and SNO-HSA (R) were 6.6 ± 0.5 and 3.3 ± 0.6 mol NO/mol HSA, respectively [23].

Cellular experiments with LY-80 cells

LY-80 Yoshida sarcoma cells (non-adherent cell), which were donated by the Institute of Development, Aging and Cancer, at Tohoku University (Sendai, Miyagi, Japan), were cultured at 37 °C in RPMI-1640 medium containing 10% fetal calf serum, 100 U/ml penicillin, and 10 μg/ml streptomycin (medium A). All cell culture experiments were performed at 37 °C in a humidified atmosphere of 5% CO_2 in air.

Changes in the mitochondrial membrane potential of LY-80 cells were monitored using flow cytometric analysis with rhodamine 123-staining. LY-80 cells (1.0×10^6 cells/well) were cultured in 12-well plates with PBS, 50 μM HSA or the indicated concentrations of SNO-HSA for 2 h. The cells then were incubated for 15 min with 10 μM rhodamine 123, followed by centrifugation at 4000 rpm for 5 min. The cell pellet was resuspended in 0.3 ml of PBS and the fluorescence intensity of rhodamine 123 in the cells was measured using a flow cytometer (FACS Calibur; Becton Dickinson Biosciences, Franklin Lakes, USA).

Caspase-3 activity was determined as follows. Cells (1.0×10^6 cells/well) were incubated in 6-well plates with medium A containing PBS, 100 μM HSA, HSA (I), SNO-HSA (R) or various concentrations of SNO-HSA. After incubation for 24 h, the cells were collected by centrifugation at 4000 rpm for 10 min and the cell pellet was washed with 0.2 ml of ice-cold PBS, followed by centrifugation. The cell pellet was resuspended in 10 μl of cell-lysis buffer. The cells were then lysed by freeze thawing, followed by a 15-min incubation on ice. The cell lysates were centrifuged at 15,000 rpm for 20 min at 4 °C, and the supernatant fraction was collected (cell extract). The caspase-3 activity in the cell extract was assessed using the colorimetric CaspASE™ Assay System (Promega, Tokyo, Japan), according to the manufacturer's instructions.

DNA degradation (DNA ladder) was detected as follows. LY-80 cells (1×10^6 cell/well) were cultured in 12-well plates with PBS, 100 μM HSA or the indicated concentrations of SNO-HSA. After incubation, culture medium containing the cells was collected and centrifuged at 4000 rpm for 5 min. After removal of the supernatant, the cell pellet was resuspended in 0.2 ml of PBS and centrifuged at 4000 rpm for 10 min. The resulting pellet was incubated in 20 μl of 10 mM Tris–HCl buffer (pH 7.8) containing 2 mM EDTA and 0.5% SDS for 10 min at 4 °C, followed by centrifugation at 15,000 rpm for 5 min. The resulting supernatant (cell extract) was collected and incubated with 1 μl of RNase A (10 μg/ml) for 30 min at 50 °C. One microliter of proteinase K (10 μg/ml) was added to the cell extract, followed by a 1-h incubation at 50 °C.

Please cite this article in press as: N. Katayama et al., Nitrosylated human serum albumin (SNO-HSA) induces apoptosis in tumor cells, Nitric Oxide (2009), doi:10.1016/j.niox.2009.09.003

The resulting DNA extract was electrophoresed in a 2.0% agarose gel, followed by staining of the gel with ethidium bromide and visualization of the DNA bands using ultraviolet illumination.

For inhibition assays, LY-80 cells were incubated for 12 h with 100 μM SNO-HSA in the absence or presence of 50 μM Z-VAD-FMK (caspase inhibitor). The extent of DNA fragmentation was determined as described above.

Cell proliferation was quantified using a Cell Counting Kit-8 (WST-8), which is based on the MTT assay. LY-80 cells were plated in 96-well plates at 1.0×10^4 cells/well and incubated for 48 h in a total volume of 0.2 ml medium A containing various concentrations of HSA or SNO-HSA. After incubation, 5 μl of WST-8 solution was added to each well and the cells were incubated for an additional 2 h at 37 °C. The number of surviving cells was determined by measurement of absorbance at 450 nm. Cell viability was calculated as a percentage of the control culture (without either HSA or SNO-HSA) [24].

For determination of lactate dehydrogenase (LDH) activity, LY-80 cells (1.0×10^4 cells/well) were incubated in 96-well plates with the indicated concentrations of HSA or SNO-HSA. After incubation for the indicated times, culture medium containing the cells was collected and centrifuged at 4000 rpm for 10 min. LDH activity in the supernatant was assessed using the LDH-Cytotoxicity Assay Kit (Bio Vision), according to the manufacturer's instructions. Cytotoxicity was calculated as a percentage based on the LDH activity released from cells that had been treated with compound compared with LDH activity from cultures incubated with Triton.

Animal experiments

Five-week-old, male Donryu rats (200–250 g) were purchased from Charles River (Nippon Charles-River Co., Ltd., Shizuoka, Japan). The rats were housed under a 12/12 h light/dark cycle in a humidity-controlled room. The rats were acclimated for at least 5 days prior to use in the experiments.

LY-80 cells (2×10^6 cells) that had been sub-cultured in the abdominal cavity of a Donryu rat were implanted in the right thigh of the experimental rats. Five days after inoculation, LY-80 sarcoma-bearing rats were randomly assigned to three groups: control (saline), HSA, and SNO-HSA. The rats received either a daily intravenous or direct intra-tumor injection of saline, HSA (10 μmol/kg), or SNO-HSA (10 μmol/kg), for 7 days (day 5–11 post-inoculation). Tumor volume was calculated using the formula 0.4 ($a \times b^2$), where 'a' is the largest and 'b' is the smallest tumor diameter [25]. Data are expressed as means ± SD. Differences between groups were evaluated using the paired Student's t-test. A p-value of less than 5% was considered to indicate a statistically significant difference.

Results

*SNO-HSA induces cell death via apoptosis **in vitro***

Mitochondria play a pivotal role in the regulation of mammalian apoptosis, which is believed to result from loss of mitochondrial membrane potential. To evaluate the effects of SNO-HSA on mitochondrial function and membrane potential, LY-80 cells were loaded with a mitochondrion-selective fluorescent cation (rhodamine 123). Compared with vehicle (PBS), SNO-HSA treatment decreased rhodamine fluorescent intensity in a dose-dependent manner. HSA also attenuated fluorescence, but to a lesser extent than SNO-HSA (Fig. 1). This observation indicates that SNO-HSA induces depolarization of the mitochondrial membrane.

Caspase-3 is a cell-death protease that is involved in the downstream execution phase of apoptosis, during which cells undergo

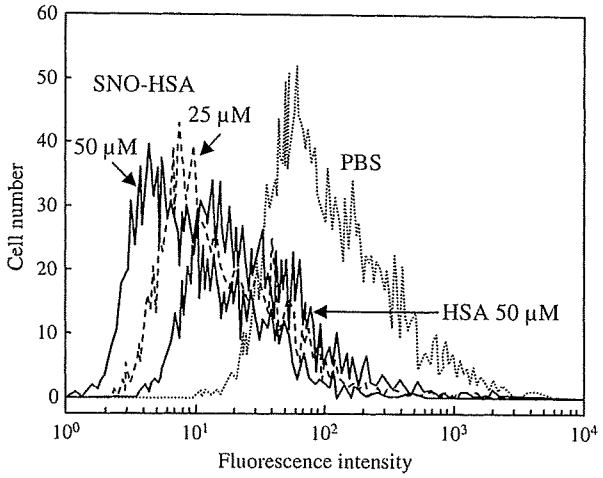

Fig. 1. Mitochondrial transmembrane potential is altered by SNO-HSA treatment. LY-80 cells were cultured with either PBS, 50 μM HSA, or various concentrations of SNO-HSA for 2 h, followed by addition of rhodamine 123. Mitochondrial transmembrane potential was analyzed using flow cytometry. Results are shown for one representative experiment.

morphological changes, such as DNA fragmentation, chromatin condensation, and formation of apoptotic bodies. Compared with vehicle-treated cultures, cells treated with 25, 50 or 100 μM SNO-HSA showed relative increases in caspase-3 activity of 21-, 34- and 42-fold, respectively. The caspase-3 activity of HSA-treated cells was equivalent to that of cells treated with PBS. In addition, in order to elucidate the effect of iminothiolane on the activation of caspase-3, HSA (I) and SNO-HSA (R) were also incubated with LY-80 cells. Surprisingly, SNO-HSA (R) as well as HSA (I) did not activate caspase-3, which suggested that iminothiolane did not participate in the activation of caspase-3 and that NO bound via functional thiols introduced by reaction of iminothiolane with terminal amines in HSA might be more efficient for its release than NO bound to terminal thiols obtained by reduction (Fig. 2). As an interesting observation supporting the result, uptake of NO from

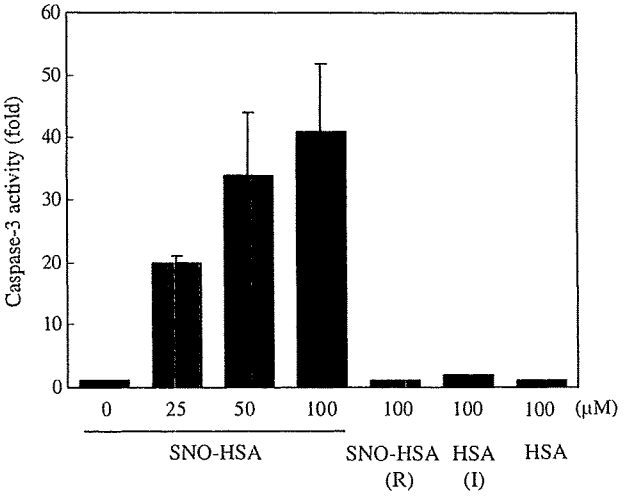

Fig. 2. Activation of caspase-3 after SNO-HSA treatment. LY-80 cells were incubated with either PBS, 100 μM HSA, HSA (I), SNO-HSA (R) or various concentrations of SNO-HSA for 24 h. Because the amounts of NO bound to SNO-HSA (R) and SNO-HSA are 6.6 ± 0.5 and 3.3 ± 0.6 mol NO/mol HSA, respectively, NO content of SNO-HSA (R) is nearly equivalent to 50 μM SNO-HSA. Caspase-3 activity was determined as described in Material and methods and is expressed as the ratio of absorbance estimated from the culture with the test compound relative to the absorbance of cultures incubated with PBS. Results are means ± SD of three separate experiments.

Please cite this article in press as: N. Katayama et al., Nitrosylated human serum albumin (SNO-HSA) induces apoptosis in tumor cells, Nitric Oxide (2009), doi:10.1016/j.niox.2009.09.003

SNO-HSA to HepG2 cell was much higher than that from SNO-HSA (R) (our unpublished observations). The mechanisms by which the difference of NO uptake between SNO-HSA and SNO-HSA (R) arose need to be investigated in future studies.

To further confirm that SNO-HSA induced apoptosis in LY-80 cells, DNA fragmentation, which is a morphological change characteristic of the execution phase of apoptosis, was examined. DNA fragmentation was observed in LY-80 cells after 4 h of incubation in 100 μM SNO-HSA and stabilized after 8 h. However, DNA fragmentation was not detected until 24 h of incubation in 100 μM HSA (Fig. 3A). Moreover, the DNA ladder observed after 12 h of incubation in SNO-HSA increased in a dose-dependent manner (Fig. 3B). To determine the mechanism by which SNO-HSA causes DNA fragmentation, LY-80 cells were simultaneously incubated with SNO-HSA and Z-VAD-FMK (a caspase inhibitor). DNA fragmentation induced by 100 μM SNO-HSA was completely abolished by treatment with Z-VAD-FMK (Fig. 3C). This result indicates that caspases are positive, upstream regulators of the DNA fragmentation that is elicited by SNO-HSA.

To determine the effect of SNO-HSA on cell growth, the viability of LY-80 cells was examined after treatment with either HSA or various concentrations of SNO-HSA. SNO-HSA inhibited growth of LY-80 cells in a concentration-dependent manner. HSA also tended to abrogate cell proliferation, but to a lesser extent than SNO-HSA (Fig. 4).

To further characterize SNO-HSA-induced LY-80 cell death, cytotoxicity was examined using an assay of LDH activity. LDH is a stable enzyme that is rapidly released from cells into the cell culture medium upon damage to the plasma membrane. Cell death increased with incubation duration for the cultures incubated with

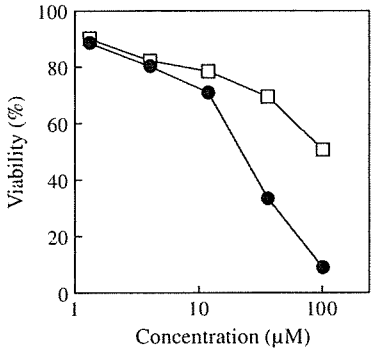

Fig. 4. Effect of SNO-HSA on cell viability. LY-80 cells were treated for 48 h with various concentrations of HSA (open squares) or SNO-HSA (closed circles). Cell viability was determined as described in Materials and methods. Results from three separate experiments are presented as means.

100 μM SNO-HSA. After 48 h of incubation, LDH was released from nearly all cells. In contrast, HSA was not cytotoxic (Fig. 5A). Furthermore, SNO-HSA was cytotoxic to LY-80 cells in a dose-dependent manner (Fig. 5B). These results suggest that SNO-HSA induced cell death via activation of an intrinsic apoptosis-signaling pathway.

SNO-HSA exerts anti-tumor effects in vivo

To investigate the anti-tumor effects of SNO-HSA *in vivo*, LY-80 tumor-bearing rats received either intravenous or direct intra-tumor injections of either saline, HSA or SNO-HSA. These treatments

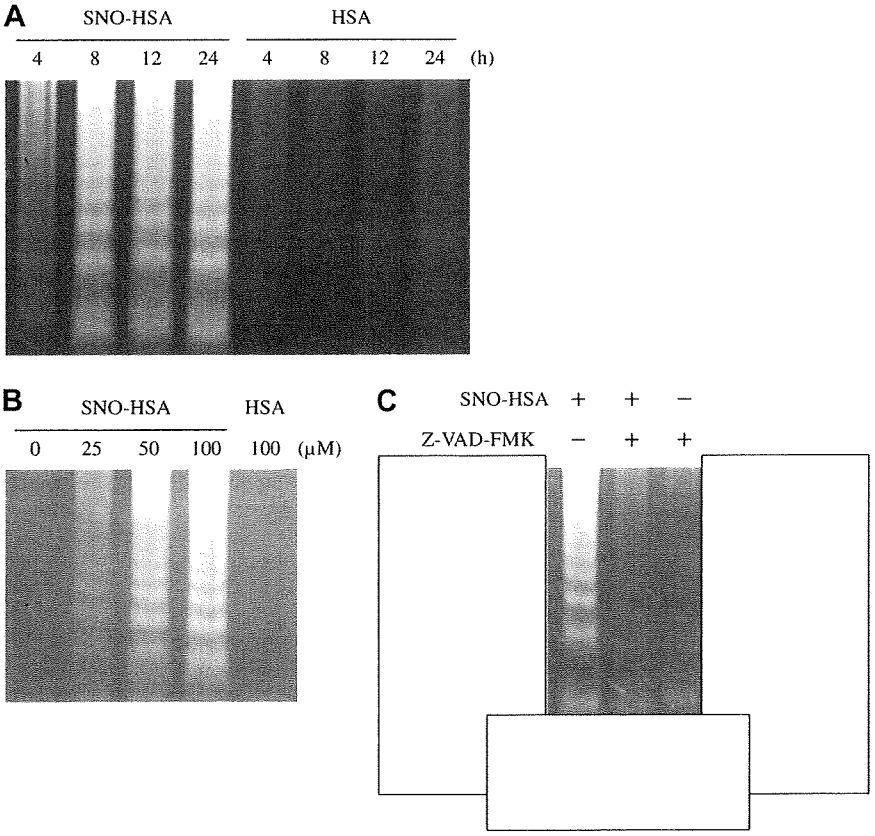

Fig. 3. DNA fragmentation after SNO-HSA treatment. (A) LY-80 cells were incubated for the indicated times with 100 μM HSA or SNO-HSA. (B) LY-80 cells were incubated for 12 h with 100 μM HSA or the indicated concentrations of SNO-HSA. (C) LY-80 cells were incubated for 12 h with 100 μM SNO-HSA in the presence or absence of 50 μM Z-VAD-FMK (caspase inhibitor). DNA fragmentation was detected as described in Materials and methods.

Please cite this article in press as: N. Katayama et al., Nitrosylated human serum albumin (SNO-HSA) induces apoptosis in tumor cells, Nitric Oxide (2009), doi:10.1016/j.niox.2009.09.003

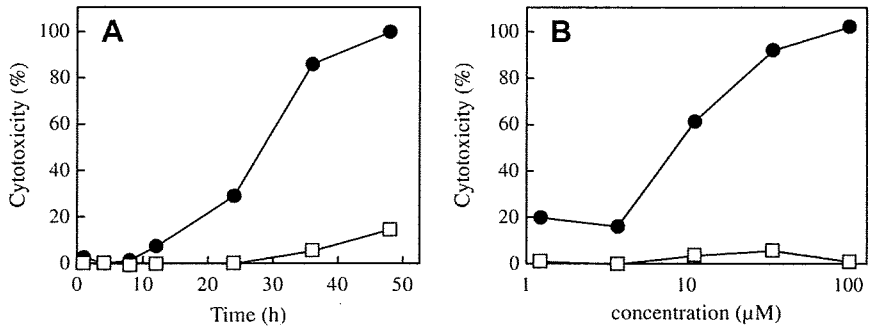

Fig. 5. Effect of SNO-HSA on LDH release (cytotoxicity). (A) LY-80 cells were incubated for the indicated times with 100 μM HSA (open squares) or SNO-HSA (closed circles). (B) LY-80 cells were treated for 48 h with various concentrations of HSA (open squares) or SNO-HSA (closed circles). LDH released from the cells was quantified as described in Materials and methods. Cytotoxicity was plotted as a percentage of total LDH release. Results from three separate experiments are presented as means.

were repeated daily for seven days (day 5–11 post-inoculation). Mean tumor volume increased with time in the saline-treated group. A similar result was also observed in the HSA-treated group. However, tumor growth in animals that received direct intra-tumor injections of SNO-HSA was only one-third that observed in the saline- and HSA-treated animals (Fig. 6). This observation suggests that SNO-HSA has anti-tumor effects *in vivo*, presumably due to induction of apoptosis. In contrast, the effects of intravenous injection of SNO-HSA on tumor growth were not significantly different from those observed with saline- and HSA-treatment (data not shown).

Discussion

We have previously reported that SNO-HSA induces intracellular changes that are characteristic of apoptosis, including mitochondrial depolarization, activation of caspase-3 and DNA fragmentation in C26 cells. In addition, intravenous injection of SNO-HSA into C26 cell-bearing mice suppressed tumor growth due to activation of the apoptotic pathway. The purpose of the present study was to evaluate the effects of SNO-HSA on a different carcinoma cell line, LY-80 cells, and to further characterize the mechanism by which SNO-HSA induces apoptosis. In the present study, SNO-HSA also elicited mitochondrial depolarization (Fig. 1), activated caspase-3 (Fig. 2) and induced DNA fragmentation (Fig. 3) in LY-80 cells. Inhibition of caspases by co-incubation with Z-VAD-FMK completely inhibited DNA fragmentation (Fig. 3C). This observation suggests that caspase activation is essential for induction of apoptosis by SNO-HSA and that these molecular events result in cell death (Figs. 4 and 5). Furthermore, injection of SNO-HSA directly into tumor tissue inhibited tumor growth in LY-80 tumor-bearing rats *in vivo*. Therefore, SNO-HSA has anti-tumor activity against LY-80 cancer cells, as well as against C26 cells.

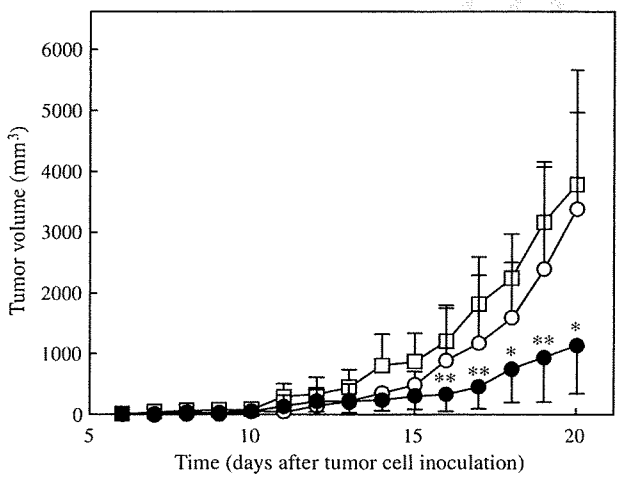

Fig. 6. Effect of SNO-HSA on tumor growth in LY-80 tumor-bearing rats. LY-80 tumor-bearing rats were given daily intra-tumor injections of saline (5 ml/kg; open squares), HSA (10 μmol/5 ml/kg; open circles) or SNO-HSA (10 μmol/5 ml/kg; closed circles) for 7 days (day 5–11 after inoculation with tumor cells). Tumor size was measured and tumor volume was calculated according to the formula: $V = 0.4a^2b$, where a is the smallest, and b the largest, superficial diameter. Results are means ± SD; $n = 4$ animals per experimental group. *Statistically significant reduction compared with saline- ($P < 0.01$) or HSA- ($P < 0.01$) treatment at the corresponding time. **Statistically significant reduction compared with saline- ($P < 0.01$) or HSA- ($P < 0.05$) treatment groups at the corresponding time.

However, *in vivo*, the effects of SNO-HSA on LY-80 cells differed from those observed for C26 cells. In the present study, direct intra-tumor injections of SNO-HSA into LY-80 tumor-bearing rats suppressed tumor growth, possibly due to induction of apoptosis. Unexpectedly, intravenous injection of SNO-HSA did not have an anti-tumor effect (data not shown). In contrast, we previously reported that tumor growth in C26 tumor-bearing mice was significantly inhibited by intravenous administration of SNO-HSA. One possible reason for the inconsistent results is that tumor blood flow might be reduced in LY-80 tumor-bearing rats compared with that in animal models of other cancers, including C26 tumor-bearing mice. Tanda et al. evaluated tumor growth in LY-80 tumor-bearing rats after intravenous administration of adriamycin (ADM) with or without dopamine (DA), which increased tumor blood flow. Despite ADM has potent anti-tumor effects of ADM, administration of ADM alone did not affect the growth of the LY-80 tumor. However, co-administration of ADM and DA inhibited tumor growth. This result suggests that delivery of substances injected intravenously is in inefficient because tumor blood flow is attenuated in LY-80 tumor-bearing rats [26]. Similarly, intravenous injection of SNO-HSA into LY-80 tumor-bearing mice might limit the anti-tumor effects of SNO-HSA. In contrast, Ogawara et al. examined the anti-tumor effects of polyethylene glycol (PEG)-modified liposomal doxorubicin (DOX) in three different tumor cell lines (Lewis lung cancer (LLC), C26 and B16BL6 melanoma (B16)) *in vitro* and *in vivo*. Although LLC exhibited the greatest sensitivity to DOX *in vitro*, the strongest *in vivo* anti-tumor effect was observed in the C26 tumor-bearing mice. Evans blue extravasation and secretion of VEGF in C26 tumors were greater than in LLC tumors [27]. These findings suggest that the vasculature in C26 tumors was more permeable than that of other tumor cell lines. Therefore, the difference in vascular permeability between LY-80

Please cite this article in press as: N. Katayama et al., Nitrosylated human serum albumin (SNO-HSA) induces apoptosis in tumor cells, Nitric Oxide (2009), doi:10.1016/j.niox.2009.09.003

and C26 tumors may be a major cause of the different response to intravenous administration of SNO-HSA. Another possible explanation is the rapid clearance of SNO-HSA *in vivo*. In our previous report, intravenous injection of SNO-HSA significantly inhibited tumor growth in C26 tumor-bearing mice, but daily injections were required to elicit a therapeutic effect. SNO-HSA is considered to be a reservoir of NO *in vivo*. HSA is the most abundant protein in plasma and it has a longer half-life than other NO donors. However, the apparent *in vivo* half-life of the S-nitroso moieties on SNO-HSA was estimated to be 18.9 min (data not shown); HSA-bound compounds are not always long-acting therapeutic agents. Therefore, rapid elimination of SNO-HSA may also explain the lack of *in vivo* activity following intravenous injection. In this context, Katsumi et al. prepared poly-NO-BSA conjugated with polyethylene glycol (PEG) and showed that, *in vitro*, the half-life of NO was 11 times longer than that of poly-NO-BSA without PEG [28]. Consequently, modification with PEG may enhance the anti-tumor activity of SNO-HSA. Furthermore, HSA molecules tend to accumulate in tumor tissues, apparently due to hypervascularization and enhanced vascular permeability (even to macromolecules) of the tumor, and minimal export of macromolecules from the tumor tissue via blood or lymphatic vessels [29]. Therefore, it was expected that SNO-HSA would enhance NO accumulation in tumors and, therefore, would be a useful agent for targeting chemotherapeutics to tumors.

In both the present study and our earlier investigation, HSA alone decreased the viability of both LY-80 cells (Fig. 4) and C26 cells compared with control cultures that were incubated without additives. In the experiment shown in Fig. 4, WST-8 is bio-reduced by cellular dehydrogenase in viable cells to produce an orange formazan product. The amount of the formazan product is directly proportional to the number of viable cells, but is not related to the ratio of living cells/total cells. Ten percent of FCS in medium A used in this experiment includes 4.1 mg/ml of proteins containing 3.3 mg/ml of albumin (~50 μM). Therefore, total amount of proteins in medium A containing 100 μM HSA reaches 10.8 mg/ml in which 10.0 mg/ml of albumin (~150 μM) is included, indicating that cells treated with 100 μM HSA are cultured at 2.6 times higher concentrations of proteins than control culture (calculated as 100% viability). Accordingly, the inhibition of cell proliferation by HSA might result from high concentrations of protein at which LY-80 cells are cultured. In contrast, in the experiment shown in Fig. 5, determination of LDH released by dead cells is indicative of the level of cellular cytotoxicity. Incubation with HSA did not result in LDH release (Fig. 5). Taken together, these observations suggest that HSA (or high concentrations of proteins) inhibits cell proliferation, but is not cytotoxic.

Although we assumed that NO plays a key role in SNO-HSA-induced apoptosis, there are many reports describing the anti-apoptotic effects of NO. The amount of NO may be one of the most potential causes for this discrepancy. The NO contents of SNO-HSA used in our studies were 6.6 mol NO/mol HSA and the S-nitroso moiety concentrations *in vitro* were 165–660 μM (25–100 μM as HSA molecule). Qiang et al. reported that high concentrations GSNO (100–300 μM) induced apoptosis and inhibited cell growth in colon cancer cell lines, such as HCA7, HT29 and HCT116 [14]. Mebmer et al. reported that apoptosis (characterized by DNA fragmentation and morphological changes) was observed in U937 cells treated with GSNO at concentrations in excess of 250 μM [30]. In contrast, NO-R410C (a genetic variant of HSA) had anti-apoptotic activity at 26–130 μM in U937 cells [31], and 10–100 μM GSNO inhibited actinomycin D-induced activation of caspase-3 in U937 cells [32]. Based on the results of the present study and those of previously published investigations, the critical NO concentration that determines if NO promotes or inhibits apoptosis appears to be 100–200 μM NO. On the other hand, SNO-HSA never inhibited the activation of caspase-3 at any concentration lower than 100 μM NO, because the activity of caspase-3 was originally little observed in LY-80 cells and thus it was difficult to detect its reduction. To resolve this issue, the effect of SNO-HSA might be needed to be investigated under conditions where caspase-3 is activated by appropriate substance.

In summary, the cytotoxic activity of NO is currently being investigated for use in anti-cancer therapies. The present study was undertaken to evaluate the anti-tumor activity of SNO-HSA in LY-80 tumor cells. SNO-HSA activated an intrinsic apoptosis-signaling pathway, resulting in cell death. In the *in vivo* experiments, direct intra-tumor injection of SNO-HSA inhibited tumor growth, while intravenous administration had no effect on tumor growth. Thus, SNO-HSA with a long half-life may be a promising candidate for cancer therapy. In addition, SNO-HSA is an endogenous substance and has few side effects, as reported previously.

References

[1] H. Okada, T.W. Mak, Pathways of apoptotic and non-apoptotic death in tumor cells, Nat. Rev. Cancer (4) (2004) 592–603.
[2] X.W. Meng, S.H. Lee, S.H. Kaufmann, Apoptosis in the treatment of cancer: a promise kept?, Curr Opin. Cell Biol. 18 (2006) 668–676.
[3] S.H. Kaufmann, G.J. Gores, Apoptosis in cancer: cause and cure, Bioessays 22 (2000) 1007–1017.
[4] Y. Kondo, T. Kanzawa, R. Sawaya, S. Kondo, The role of autophagy in cancer development and response to therapy, Nat. Rev. Cancer 5 (2005) 726–734.
[5] B. Brune, K. Sandau, A.V. Knethen, Apoptotic cell death and nitric oxide: activating and antagonistic transducing pathways, Biochemistry (Mosc.) 63 (1998) 817–825.
[6] S. Moncada, A. Higgs, The L-arginine–nitric oxide pathway, N. Engl. J. Med. 329 (1993) 2002–2012.
[7] L.J. Ignarro, Endothelium-derived nitric oxide – pharmacology and relationship to the actions of organic nitrate esters, Pharmacol. Res. 6 (1989) 651–659.
[8] H. Azuma, M. Ishikawa, S. Sekizaki, Endothelium-dependent inhibition of platelet aggregation, Br. J. Pharmacol. 88 (1986) 411–415.
[9] J. Garthweite, Glutamate, nitric oxide and cell–cell signaling in the nervous system, Trends Neurosci. 14 (1991) 60–67.
[10] M.A. Marletta, P.S. Yoon, R. Iyengar, C.D. Leaf, J.S. Wishnok, Macrophage oxidation of L-arginine to nitrite and nitrate–nitric oxide is an intermediate, Biochemistry 27 (1988) 8706–8711.
[11] F. Laval, D.A. Wink, Inhibition by nitric oxide of the repair protein, O6-methylguanine-DNA-methyltransferase, Carcinogenesis 15 (1994) 443–447.
[12] J.B. Hibbs Jr., R.R. Taintor, Z. Vavrin, E.M. Rachlin, Nitric oxide: a cytotoxic activated macrophage effector molecule, Biochem. Biophys. Res. Commun. 157 (1988) 87–94.
[13] J.S. Beckman, J.P. Crow, Pathological implication of nitric oxide, superoxide and peroxnitrite formation, Biochem. Soc. Trans. 21 (1993) 330–334.
[14] L. Qiang, S.T.F. Chan, R. Mahendran, Nitric oxide induces cyclooxygenase expression and inhibits cell growth in colon cancer cell lines, Carcinogenesis 24 (2003) 637–642.
[15] F. Fabbri, G. Brigliadori, P. Ulivi, A. Tesei, I. Vannini, M. Rosetti, S. Bravaccini, D. Amadori, M. Bolla, W. Zoli, Pro-apoptotic effect of a nitric oxide-donating NSAID, NCX4040, on bladder carcinoma cells, Apoptosis 10 (2005) 1095–1103.
[16] K. Kashifi, Y. Ryann, L.L. Qiao, J.L. Williams, J. Chen, P.D. Soldato, F.T. Traganos, B. Rigas, Nitric oxide-donating nonsteroidal anti-inflammatory drugs inhibit the growth of various cultured human cancer cells: evidence of a tissue type-independent effect, J. Pharmacol. Exp. Ther. 303 (2002) 1273–1282.
[17] J.L. Williams, S. Borgo, I. Hasan, E. Castillo, F. Traganos, B. Rigas, Nitric oxide-releasing nonsteroidal anti-inflammatory drugs (NSAIDs) alter the kinetics of human colon cancer cell lines more effectively than traditional NSAIDs: implication for colon cancer chemoprevention, Cancer Res. 61 (2001) 3285–3289.
[18] J.S. Stamler, O. Jaraki, J. Osborne, D.I. Simon, J. Keaney, J. Vita, D. Singel, C.R. Valeri, J. Loscalzo, Nitric oxide circulates in mammalian plasma primarily as an S-nitroso adduct of serum albumin, Proc. Natl. Acad. Sci. USA 89 (1992) 7674–7677.
[19] T. Peters Jr., Serum albumin, Adv. Protein Chem. 37 (1985) 161–245.
[20] N. Katayama, K. Nakajou, H. Komori, K. Uchida, J.I. Yokoe, N. Yasui, H. Yamamoto, T. Kai, M. Sato, T. Nakagawa, M. Takeya, T. Maruyama, M. Otagiri, Design and evaluation of S-nitrosylated human serum albumin as a novel anticancer drug, J. Pharmacol. Exp. Ther. 325 (2008) 69–76.
[21] S. Matsushita, Y. Ishima, V.T. Chuang, H. Watanabe, S. Tanase, T. Maruyama, M. Otagiri, Functional analysis of recombinant human serum albumin domains for pharmaceutical applications, Pharm. Res. 10 (2004) 1924–1932.
[22] R.F. Chen, Removal of fatty acids from serum albumin by charcoal treatment, J. Biol. Chem. 242 (1967) 173–181.
[23] A.F. Habeeb, Determination of free amino groups in proteins by trinitrobenzene–sulfonic acid, Anal. Biochem. 14 (1966) 328–336.
[24] M. Ishiyama, H. Tominaga, M. Shiga, K. Sasamoto, Y. Ohkura, K. Ueno, A combined assay of cell viability and in vitro cytotoxicity with a highly water-

Please cite this article in press as: N. Katayama et al., Nitrosylated human serum albumin (SNO-HSA) induces apoptosis in tumor cells, Nitric Oxide (2009), doi:10.1016/j.niox.2009.09.003

soluble tetrazolium salt, neutral red and crystal violet, Biol. Pharm. Bull. 19 (1996) 1518–1520.
[25] K. Shimizu, T. Asai, C. Fuse, Y. Sadzuka, T. Sonobe, K. Ogino, T. Taki, T. Tanaka, N. Oku, Applicability of anti-neovascular therapy to drug-resistant tumor: suppression of drug-resistant P388 tumor growth with neovessel-targeted liposomal adriamycin, Int. J. Pharm. 296 (2005) 133–141.
[26] S. Tanda, K. Hori, Q.H. Zhang, H.C. Li, M. Suzuki, Effects of intravenous infusion of dopamine on tumor blood flow in rats subcutis, Jpn. Cancer Res. 85 (1994) 556–562.
[27] K.I. Ogawara, K. Un, K. Minato, K.I. Tanaka, K. Higaki, T. Kimura, Determinants for in vivo anti-tumor effects of PEG liposomal doxorubicin: importance of vascular permeability within tumors, Int. J. Pharm. 359 (2008) 234–240.
[28] H. Katsumi, M. Nishikawa, F. Yamashita, M. Hashida, Development of polyethylene glycol-conjugated poly-s-nitrosated serum albumin, a novel s-nitrosothiol for prolonged delivery of nitric oxide in the blood circulation in vivo, J. Pharmacol. Exp. Ther. 314 (2005) 1117–1124.
[29] Y. Matsumura, T. Oda, H. Maeda, General mechanism of intratumor accumulation of macromolecules: advantage of macromolecular therapeutics, Jpn. J. Cancer Chemother. 14 (pt. II) (1987) 821–829.
[30] U.K. Mebmer, D.M. Reimer, B. Brune, Nitric oxide-induced apoptosis: p53-dependent and p53-independent signaling pathways, Biochem. J. 319 (1995) 299–305.
[31] Y. Ishima, T. Sawa, U. Kragh-Hansen, Y. Miyamoto, S. Matsushita, T. Akaike, M. Otagiri, S-nitrosylation of human variant albumin Liprizzi (R410C) confers potent antibacterial and cytoprotective properties, J. Pharmacol. Exp. Ther. 320 (2007) 969–977.
[32] S. Mohr, B. Zech, E.G. Lapetina, B. Brune, Inhibition of caspase-3 by S-nitrosation and oxidation caused by nitric oxide, Biochem. Biophys. Res. Commun. 238 (1997) 387–391.

Please cite this article in press as: N. Katayama et al., Nitrosylated human serum albumin (SNO-HSA) induces apoptosis in tumor cells, Nitric Oxide (2009), doi:10.1016/j.niox.2009.09.003

Effect of Reactive-Aldehydes on the Modification and Dysfunction of Human Serum Albumin

KATSUMI MERA,[1] KAZUHIRO TAKEO,[1] MIYOKO IZUMI,[1] TORU MARUYAMA,[1,2] RYOJI NAGAI,[3] MASAKI OTAGIRI[1,4]

[1]Department of Biopharmaceutics, Graduate School of Pharmaceutical Sciences, Kumamoto University, Kumamoto, Japan

[2]Center for Clinical Pharmaceutical Science, Kumamoto University, Kumamoto, Japan

[3]Department of Food and Nutrition, Laboratory of Nutritional Science and Biochemistry, Japan Women's University, 2-8-1 Mejirodai, Bunkyo-ku, Tokyo 112-8681, Japan

[4]Faculty of Pharmaceutical Sciences, Sojo University, Japan

Received 14 April 2009; revised 15 July 2009; accepted 4 August 2009

Published online 16 September 2009 in Wiley InterScience (www.interscience.wiley.com). DOI 10.1002/jps.21927

ABSTRACT: Advanced glycation end products (AGEs) are generated not only from glucose but also from several aldehydes such as methylglyoxal, glyoxal, and glycolaldehyde. The aim of the present study was to investigate the effect of several aldehydes on human serum albumin (HSA) in terms of the physicochemical properties and formation of AGE structures. HSA modified with methylglyoxal, generated by the glycolysis pathway and degradation of the Schiff base, showed the highest increase in the molecular weight and net negative charge, whereas glucose modification caused a small increase in the molecular weight even incubation for after 4 weeks. N^{ε}-(carboxymethyl)-lysine (CML), N^{ε}-(carboxyethyl)lysine (CEL), and imidazolone increased in modified HSA in correlation with their lysine and arginine modification, whereas high amounts of GA-pyridine was detected in HSA modified with glycolaldehyde. Furthermore, the binding ability of HSA to warfarin and ketoprofen was more effectively decreased by methylglyoxal modification than the other aldehydes. These results indicated that changes in the physicochemical properties and the formation of AGE structures are highly dependent on the aldehydes. © 2009 Wiley-Liss, Inc. and the American Pharmacists Association J Pharm Sci 99:1614–1625, 2010

Keywords: albumin; distribution; drug interactions; protein binding; protein aggregation

INTRODUCTION

Reducing sugars such as glucose and ribose nonenzymatically react with amino residues of proteins to form Schiff base and Amadori products. Further incubation converts these early products into irreversible derivatives termed advanced glycation end products (AGEs). Protein modification by glucose results in the induction of the functional disruption of proteins such as human serum albumin (HSA),[1,2] alpha-crystalline,[3] and copper–zinc-superoxide dismutase.[4] Furthermore, recent studies have demonstrated that AGEs are generated not only from glucose but also from aldehydes such as glyoxal, methylglyoxal,[5] glucosone,[6] and glycolaldehyde,[7] and those aldehydes rapidly modify proteins. For instance, Mclellan et al.[8] demonstrated that plasma methylglyoxal concentrations in insulin-dependent diabetic patients were seven-times

Additional Supporting Information may be found in the online version of this article.

Abbreviations: AGE(s), advanced glycation end products; HSA, human serum albumin; CML, N^{ε}-(carboxymethyl)lysine; CEL, N^{ε}-(carboxyethyl)lysine; CMA, N^{ω}-(carboxymethyl)arginine; 3DG, 3-deoxyglucosone; ELISA, enzyme-linked immunosorbent assay; PBS, phosphate-buffered saline.

Katsumi Mera and Kazuhiro Takeo contributed equally to this work.

Correspondence to: Ryoji Nagai (Telephone: +81-3-5981-3430; Fax: +81-3-5981-3430; E-mail: nagai-883@umin.ac.jp)

Journal of Pharmaceutical Sciences, Vol. 99, 1614–1625 (2010)

higher than those of healthy individuals. Furthermore, thiamine and its derivative, benfotiamine, are known to decrease methylglyoxal level *in vivo* and inhibit the development of incipient nephropathy[9] and retinopathy[10] in streptozotocin-induced diabetic rats. Glycolaldehyde is generated by the reaction of hypochloric acid with serine, and reacts with proteins to form AGEs such as N^{ε}-(carboxymethyl)lysine (CML)[11,12] and GA-pyridine[7] which accumulate in human atherosclerotic lesions. These reports indicate that the modification of proteins with aldehydes *in vivo* may contribute to the pathogenesis of diabetic complications by enhancing posttranslational modification in various human tissues. However, little is known about the difference of physicochemical properties and formed AGE structures among aldehydes-modified proteins since most of previous immunochemical studies using anti-AGE antibodies were used conventional antibodies which were cross-reactive with those analogues[13] or those epitopes are unidentified.[14] A production system has been developed to make monoclonal antibodies against several AGE structures.[15–17]

The present study measured the effects of protein modification by several aldehydes on the denaturalization and function of proteins. HSA was selected to measure the role of aldehydes in protein modification, because it is the most abundant protein in human blood plasma and the major target for glycation and oxidation among plasma proteins.[18,19] Our results demonstrated that an increase in the negative charge and formed AGEs are dependent on each aldehyde and that modification of arginine may be an important factor for the binding of drugs such as warfarin and ketoprofen to HSA.

MATERIALS AND METHODS

Chemicals

HSA was donated by the Chemo-Sera-Therapeutic Research Institute (Kumamoto, Japan) and was defatted using charcoal treatment as described by Chen[20]. D-glucose, methylglyoxal, glyceraldehydes, and glycolaldehyde were purchased from Sigma (St. Louis, MO). Glyoxal was obtained from Nacalai Tesque (Kyoto, Japan). Horseradish peroxidase (HRP)-conjugated goat anti-mouse IgG antibody was purchased from Kirkegaard Perry Laboratories (Gaitherburg, MD). Glucosone[21] and 3-deoxyglucosone (3DG)[22] were prepared according to a previously published method. All other chemicals were of the best grade available from commercial sources.

Preparation of Aldehyde-Modified HSA

To prepare the methylglyoxal-modified HSA (methylglyoxal-HSA), glyoxal-modified HSA (glyoxal-HSA), glyceraldehyde-modified HSA (glyceraldehyde-HSA), and glycolaldehyde-modified HSA (glycolaldehyde-HSA), 2 mg/mL HSA was incubated with 10 mM of methylglyoxal, glyoxal, glyceraldehydes, or glycolaldehydes at 37°C for up to 7 days in 100 mM sodium phosphate buffer (pH 7.4). To prepare the glucose-modified HSA (glucose-HSA) and 3DG-modified HSA (3DG-HSA), 2 mg/mL HSA was incubated with 10 mM of D-glucose or 3DG at 37°C for up to 4 weeks in 100 mM sodium phosphate buffer (pH 7.4). To prepare the glucosone-modified HSA (glucosone-HSA), 2 mg/mL HSA was incubated with 10 mM of glucosone at 37°C for up to 4 weeks in 100 mM HPES buffer (pH 7.4). The aliquots were obtained from each reaction mixture and dialyzed against phosphate-buffered saline (PBS).

The Molecular Mass of Aldehyde-Modified HSA

The molecular mass of the aldehyde-modified HSA was measured as described previously.[23] Briefly, 1 μL of the sample protein solution (10 μM) in 0.1% aqueous trifluoroacetic acid (TFA) water was applied on a sample spot in a steel plate slide and dried in a stream of warm air. The matrix solution which contained 10 mg/mL 3,5-dimethoxy-4-hydroxycinnanic acid (sinapinic acid; Sigma–Aldrich, Tokyo, Japan) in 50% (v/v) ethanol in 0.1% (v/v) TFA was applied on a dried sample spot then dried in a stream of warm air again. The molecular mass of the sample was analyzed by Matrix Assisted Laser Desorption/Ionization-Time of Flight Mass Spectrometry (MALDI-TOFMS; Shimadzu/Kratos Kompact MALDI III mass spectrometer, Kyoto, Japan), which was operated in the positive high-energy linear mode.

Agarose Gel Electrophoresis

An agarose gel electrophoresis was performed using the Universal Gel/8 electrophoresis kit

(Ciba-Corning, Tokyo, Japan), followed by staining with Coomassie brilliant blue. The electrophoretic mobility of the aldehyde-modified HSA relative to native HSA were expressed as the relative electrophoretic mobility.

Amino Acid Analysis

The amino acid composition of the aldehyde-modified HSA was quantified by performing amino acid analysis after acid hydrolysis with 6 N HCl for 24 h at 110°C. Amino acids were analyzed with an amino acid analyzer (Model 835; Hitachi, Tokyo, Japan) using an ion exchange high-performance liquid chromatography column (number 2622 SC, 4.6 mm × 60 mm; Hitachi) and the ninhydrin postcolumn detecting system. The modification ratios of lysine and arginine residues were also estimated by spectroscopic methods. The extent of lysine modification on proteins was determined by reaction with 2,4,6-trinitrobenzenesulfonic acid (TNBS)[24] using unmodified HSA as the calibration standard. Briefly, 200 μL of 0.2 mol/L borate (pH 9.0) and 80 μL of 15 mmol/L TNBS were added to 200 μL of each sample. After incubation at 37°C for 30 min, the reaction was terminated by adding 800 μL 90% formic acid followed by measurement of absorbance at 420 nm. The arginine modification ratio was determined by 9,10-phenanthrenequinone.[25,26] Briefly, modified HSA preparations in 50 mmol/L sodium borate (pH 8.5) were incubated at 37°C for 5 h with 37.5 μmol/L of 9,10-phenanthrenequinone and 0.25 mol/L sodium hydroxide. An equal volume of 1 mol/L hydrochloric acid was added to terminate the reaction, and fluorescence intensity (excitation, 312 nm; emission, 395 nm) was measured. The modification ratio of each sample was expressed as the percent of modification with unmodified HSA as a control.

Enzyme-Linked Immunosorbent Assay

An enzyme-linked immunosorbent assay (ELISA) was performed as described previously.[27] Briefly, each well of a 96-well microtiter plate was coated with 100 μL of the indicated concentration of sample in PBS, and incubated for 2 h. The wells were washed three times with PBS containing 0.05% Tween-20 (washing buffer), then blocked with 0.5% gelatin in PBS for 1 h. After washing three times, the wells were incubated for 1 h with 100 μL of the primary antibody including monoclonal anti-AGE antibody (6D12: 0.5 μg/mL),[13] monoclonal anti-CML antibody (2G11: 1 μg/mL),[15] monoclonal anti-N^{ε}-(carboxyethyl)lysine (CEL) antibody (CEL-SP: 5 μg/mL),[17] monoclonal anti-GA-pyridine antibody (2A2: 0.5 μg/mL),[28] monoclonal anti-imidazolone antibody (JNH-27: 1 μg/mL)[29,30] and monoclonal anti-pyrraline antibody (H-12: 10 μg/mL).[29] After triplicate washing, the wells were incubated with HRP-conjugated anti-mouse IgG, followed by reaction with 1,2-phenylenediamine dihydrochloride. The reaction was terminated with 100 μL of 1.0 M sulfuric acid, and monitored using absorbance at 492 nm with a micro-ELISA plate reader (TECAN Spectra Fluor Plus, Kanagawa, Japan). JNH-27 reacts with 3DG-imidazolone and MG-imidazolone, while its reactivity with imidazole and 4-(hydroxymethyl)imidazole hydrochloride was negligible.[30] Although the quantification of AGEs by instrumental analyses is superior to immunological analyses, anti-AGE antibodies can be a convenient means for estimating the AGE contents.

Drug Binding Properties

The binding of warfarin (5 μM) and ketoprofen (5 μM) to the aldehyde-modified HSA (10 μM) in PBS (pH 7.4) was examined by ultrafiltration. The unbound ligand fractions were separated using an Amicon MPS-1 micropartition system with YMT ultrafiltration membranes by centrifugation (2000*g*, 40 min). The concentration of unbound ligand was determined by HPLC.[31,32]

RESULTS

Physicochemical Properties of Aldehyde-Modified HSA

The increase in the molecular weight of aldehyde-modified HSA was measured by a MALDI-TOFMS analysis. As shown in Figure 1A and B, the molecular mass of methylglyoxal-HSA incubated for 7 days was ~4000 Da larger than native-HSA. A time-dependent increase in molecular mass was observed in HSA modified by reactive aldehydes (Fig. 1C), whereas that of glucose-HSA was negligible even after 4 weeks of incubation (Fig. 1D). The net negative charge of aldehyde-modified HSA was determined by an agarose gel electrophoresis. Electrophoretic mobilities of aldehyde-modified HSA, especially

DOI 10.1002/jps

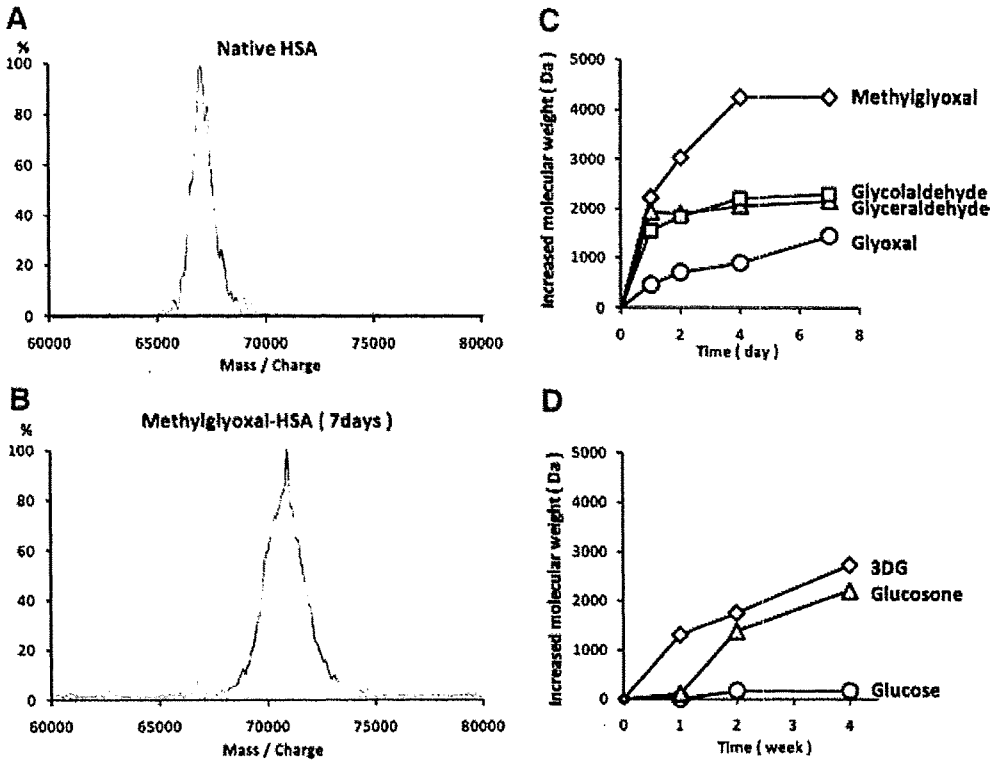

Figure 1. Molecular mass of aldehyde-modified HSA. MALDI-MS spectrometry of native HSA (A) and methylglyoxal-HSA (B). The increased molecular weight of aldehyde-modified HSA with respect to native HSA (C and D). The molecular mass of the sample was analyzed by a MALDI III mass spectrometer as described in the Materials and Methods Section.

glyceraldehyde-HSA (Fig. 2C) and glycolaldehyde-HSA (Fig. 2D), were significantly higher than those of unmodified HSA, whereas the change in glucose-HSA was small (Fig. 2G). This result indicates that the modification of HSA with reactive aldehydes increases the molecular mass and negative charge more than that with glucose.

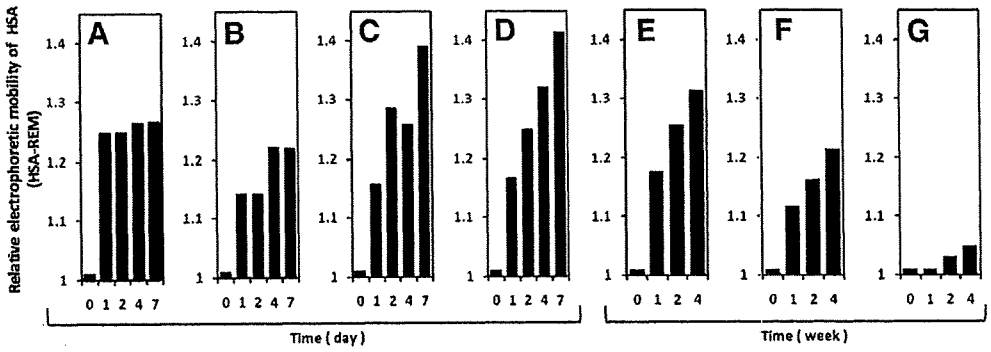

Figure 2. Net negative charge of aldehyde-modified HSA. Methylglyoxal- (A), glyoxal- (B), glyceraldehyde- (C), and glycolaldehyde-HSA (D) were prepared by incubation for 7 days, and glucose- (E), glucosone- (F), and 3DG-HSA (G) were also prepared by incubation for 4 weeks. The samples were subjected to agarose gel electrophoresis and stained with Coomassie brilliant blue. Their electrophoretic mobilities relative to native HSA were expressed as the relative electrophoretic mobility (HSA-REM).